Idaho National Engineering Laboratory

Managed by the U.S. Department of Energy

EGG-MS-8425
March 1989

INFORMAL REPORT

NDE OF THE SPACE SHUTTLE ORBITER THERMAL PROTECTION SYSTEM - PHASE II FINAL REPORT

D. M. Tow
B. A. Barna
J. G. Rodriguez

EG&G Idaho

Work performed under DOE Contract No. DE-AC07-76ID01570

EGG-MS--8425

DE89 010975

NDE OF THE SPACE SHUTTLE ORBITER THERMAL PROTECTION SYSTEM - PHASE II FINAL REPORT

D. M. Tow
B. A. Barna
J. G. Rodriguez

February 1989

EG&G Idaho, Inc.
Idaho Falls, Idaho, 83415-2209

Prepared for the
John F. Kennedy Space Center,
NASA,
through
U.S. Department of Energy
Idaho Operations Office
Under DOE Contract No. DE-AC07-76ID01570

ABSTRACT

Research continued on the development of a nondestructive evaluation technique for inspecting bonds on the space shuttle orbiter thermal protection system tiles. The approach taken uses a noncontacting laser sensor to measure the vibrational response of bonded tiles to acoustical excitation. Laboratory work concentrated on investigating the dynamic response of "acreage" tiles, i.e., tiles covering the underside of the orbiter, all approximately square. A number of promising unbond signatures have been identified in the time and frequency domain response. Field tests were conducted to study environmental effects on the techniques being developed. The ambient motion of the orbiter was found to be larger than expected, necessitating modifications to current techniques.

SUMMARY

Phase II of this research to develop a viable NDE technique for the inspection of the space shuttle orbiter thermal protection system (TPS) tile bonds has resulted in several significant accomplishments. The research methods employed in this phase are a refinement of those used in Phase I; a noncontacting laser sensor was used to measure the vibrational response of tiles to acoustical excitation. This phase concentrated on developing an empirical understanding of the bonded and unbonded vibration signatures of the acreage tiles that cover the underside of the orbiter. These tiles are all approximately square with similar dimensions. Controlled experiments using identical acreage tiles provided by Lockheed have found several candidate signatures common to all these tiles. This degree of consistency in the tile dynamic response proves that an unbond can be detected for a known tile and establishes the basis for extending the analysis capability to arbitrary tiles for which there is no historical data.

Field tests of the noncontacting laser acoustic sensor system were also conducted to establish the vibrational environment of the Orbiter Processing Facility (OPF) and its effect on the measurement and analysis techniques being developed. The data collected showed that on orbiter locations such as the body flap and elevon, the data analysis scheme and/or the sensor will require modification to accommodate the ambient motion. Several methods for accomplishing this have been identified. It was established that the tile response in the field is similar to that observed in the laboratory. Of most importance, however, is that the field environment will not affect the physics of the dynamic response that is related to bond condition. All of this information is fundamental to any future design and development of a prototype tile inspection system.

The results of this phase of work indicate that the technology being developed will ultimately be capable of verifying bond integrity on some or all of the TPS tiles. It is even possible to define best and worst case prospects for such a system at this point. The optimal case would be a system that could completely verify the bond integrity on any arbitrary tile

without benefit of previous history. The minimal system would allow bond verification of newly bonded tiles and tiles on which a history of the vibration signature had been collected.

CONTENTS

FIGURES

TABLE

NDE OF THE SPACE SHUTTLE ORBITER THERMAL PROTECTION SYSTEM - PHASE II FINAL REPORT

INTRODUCTION

It is necessary to nondestructively evaluate the bond integrity of the thermal protection system (TPS) tiles of the space shuttle orbiter. Repeated missions can degrade the bond integrity through heat and moisture degradation of the elements in the bonding system. Due to the unique nature of the fiber composite tile and the flexible strain isolation pad (SIP), conventional NDE techniques are inadequate. Discussions between National Aeronautics and Space Administration - Kennedy Space Center (NASA-KSC) and the Idaho National Engineering Laboratory (INEL) in late 1984 led to a phased research program to investigate whether approaches developed at the INEL in other work could be reduced to a practical inspection technology. Work was begun on the project in February 1986.

Three important conclusions resulted from Phase I work on this project:

1. Noncontacting acousto-optic sensing is a feasible means of measuring the vibrational response of the TPS tiles to acoustical excitation.

2. Unbonds affect the vibrational response in a measurable way.

3. Small variations in tile geometry result in quite different response characteristics.

Phase II of this project had two basic objectives:

1. Continue development of the sensing technology to the point where preliminary field measurements on the Orbiter could be made.

2. Advance the state of understanding of the physics of tile vibration and vibration measurement to the point where an informed decision could be made whether or not the approach is viable for field detection of real flaws on the Orbiter TPS.

These goals were both achieved. This report discusses the work performed during Phase II and proposes objectives for Phase III.

DEVELOPMENT OF ACOUSTO-OPTIC TECHNIQUES

Phase II has seen important progress in the area of sensor development. There is now a much better understanding of the sensor capabilities and limitations. The sensor response has been modeled and verified with experiments using the piezo pusher. In addition to this, a long focal length lens has been developed which allows data collection from up to 10 m away.

Understanding Sensor Response

The laser cavity response to light scattered from vibrating surfaces has been successfully modeled. The model is being used to study improved methods for extracting the vibration signal. The model has also been used to explain several characteristics of the signal that arise when the vibration amplitude exceeds half the light wavelength. This understanding will result in improved performance of the existing hardware and possibly development of an improved servo scheme that will allow the sensor to accommodate large amplitude vibrations, such as the ambient vibrations encountered in the Orbiter Processing Facility (OPF).

Under most conditions the sensor response can be approximated by:

$$v = A + B\cos(2k[s + \delta s])$$

where

- v is the measured voltage of the laser servo mechanism,
- A and B are constants,
- k is the angular wavenumber,
- s is the distance to the sample at rest, and
- δs is the vibrational displacement of the sample.

Rewriting the equation as

$$v = \cos(2ks)\cos(2k\delta s) - \sin(2ks)\sin(2k\delta s),$$

it is clear that v will be linearly proportional to displacement, δs, only when (a) δs is small compared to the wavelength of light and (b) the distance to the sample at rest, s, obeys the following condition:

$$s = (N + \tfrac{1}{2})\pi/2k \ .$$

That is, s is an integral number of quarter wavelengths plus 1/8 wavelength. If these criteria are met, then the equation for the sensor response becomes

$$v = -2k\delta s(-1)^N \ .$$

If the criteria are violated, then nonlinear effects are predicted. These predicted effects have been observed. Frequency doubling has been observed when the vibration displacement, δs, approaches the magnitude of a wavelength of laser light. Signal attenuation and frequency doubling are observed when the "at rest" distance to the sample violates the condition described above.

This understanding of the cavity response of the laser sensor has led to an understanding of the problems associated with collecting data from surfaces with large ambient vibration. With this understanding, methods can and have been formulated for dealing with these problems. An external cavity scheme has been proposed that would keep the optical path length to the target constant. This would ensure that the laser is always at its linear operating point. A scheme for collecting data only at turn around points in the ambient motion has also been proposed.

Long Focal Length Optics

A most important development was the implementation of a lensing arrangement that allows up to 10 m of working distance between the tiles and the measurement system. This was accomplished by increasing the focal length of the optics while maintaining equivalent light gathering capabilities. In order to obtain an adequate signal using the frequency stabilized HeNe laser, an adequate amount of light must be collected. In addition, the sensing beam must be focused to a spot size at the tile surface that is small enough to avoid averaging out of the displacement over the spot diameter.

The initial data collection was accomplished using a 100 mm focal length lens. This particular lens provided an adequate signal-to-noise ratio and the data collected with it establish a baseline optical collection capability. The calculated values of this baseline are a spot size (beam waist) at the tile surface of 102 μm and a collection capability of f/125.

The problem in achieving a long standoff distance is essentially one of imaging the primary beam waist (located within the lasing cavity) at the tile surface. Therefore, it can be seen that the problem is one of magnification. In evaluating this situation the previously mentioned criteria for adequate signal production must be kept in mind. The optical configuration for the long standoff accordingly uses two elements, a -5 mm focal length lens and a 150 mm compound lens. The -5 mm focal length lens produces a virtual beam waist with a 6.5 μm diameter and simultaneously shortens the Rayleigh range of the laser, allowing the beam waist to be imaged at the tile surface with a small diameter. Using the compound lens, the virtual beam waist is imaged at the tile surface with a calculated diameter of 124 μm. The combined effect of the two optical elements is to produce a small spot size at the tile with a collection capability of f/149 and a standoff of approximately 2 m. In addition to these properties, this configuration has a variable focal length capability allowing the lens to be used from as close as 1 m to distances greater than 9 m.

There are some slight differences for the calculated spot sizes and f-numbers between the previous single lens system and the long standoff system. These differences can be accepted since the calculations are for ideal lenses with the 150 mm compound lens considered a single thin lens for computational ease. Data collected with the long standoff lens at a variety of distances from the tile surface have been in excellent agreement with data collected using the 100 mm focal length lens.

Fielding an inspection system will be much easier because of the new lensing arrangement. The wide range in the standoff distance provides for easy access to more orbiter surfaces. Additionally, focusing is facilitated by the presence of the compound lens. Autofocusing will be easy to implement using a servo mechanism to position the focusing ring.

TILE RESPONSE STUDIES

The goal of the tile response studies was to develop an empirical understanding of the bonded and unbonded vibration signatures of the acreage tiles that cover the underside of the orbiter. These tiles are all approximately square with similar dimensions. The experimental approach concentrated on controlled unbonding experiments using "pedigree" tiles provided by Lockheed. These tiles have identical geometry and were made from the same batch of silica fibers. These tiles were used to reduce effects due to differences in tile geometry. A limited number of unbond geometries were simulated with a vacuum mounting fixture specially designed for this project. The experimental work clearly shows that bond condition affects tile response in consistent and quantifiable ways.

This section first describes the vacuum mounting fixture, and then presents the experimental results. A number of candidate unbond signatures have been identified and are discussed. The effects of a number of factors other than bond condition - filler bar, glass coating, water ingress, and strain isolation pad (SIP) aging - are also addressed. A brief description of some preliminary modeling attempts concludes this section. Only limited efforts have so far been devoted to modeling the vibrational response of the tile/SIP system. The discussion of modeling stresses the importance of useful physical models for interpreting results and predicting tile behavior. An expanded role is anticipated for modeling in future research.

Vacuum Chuck

During Phase I unbonds were simulated by first bonding the tile to an aluminum plate and then slicing through regions of the SIP with a razor blade to mimic unbonds. An easier and more repeatable method of simulating unbonds was needed, so a vacuum chuck for easy simulation of unbonds was developed during Phase II. The vacuum chuck is an aluminum plate with a nearly square array of vacuum holes, slightly smaller than the 5 x 5 in. SIP (Figure 1). When the SIP is mounted backwards on a tile, such that the RTV side faces out, the tile can be securely held by placing the RTV-sealed SIP against the face of the chuck and drawing a vacuum. Unbonds are simulated by taping over

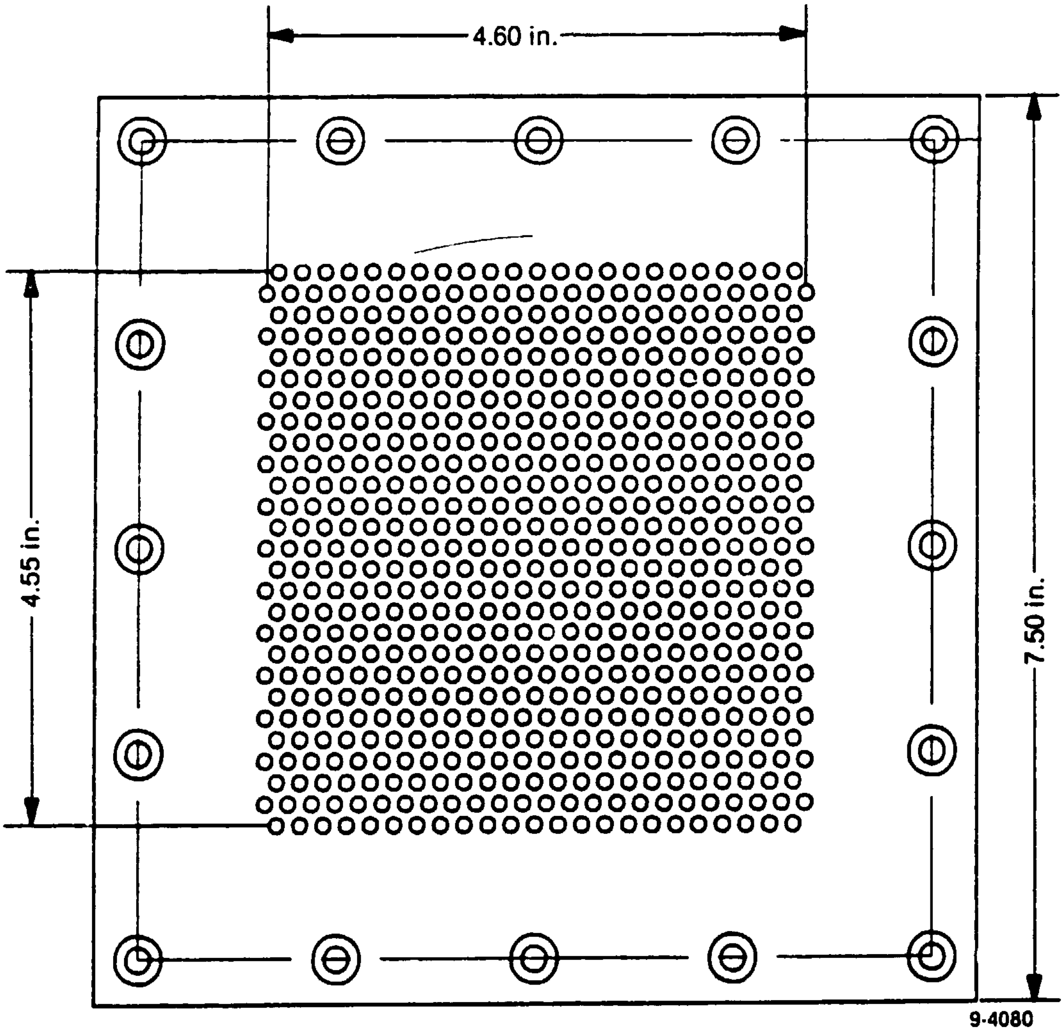

Figure 1. Vacuum chuck.

regions of vacuum holes. Tests were conducted to determine the repeatability of tile response with bonds simulated using the vacuum chuck. Tiles mounted on the vacuum chuck and remounted a few weeks later showed essentially the same dynamic response. One such result is shown in Figure 2, a display of spectra from the center point of tile 8122 collected three weeks apart.

The effect of vacuum strength on tile response was also investigated. Figure 3 shows that dynamic response is not seriously affected by drops in vacuum of a few inches of mercury. Figure 3a shows spectra from tile 8122 as vacuum is reduced, Figure 3b shows timc series data. This information provides assurance that variations in response characteristics are due to changes in bond condition, not to variations in vacuum strength from one mounting to another.

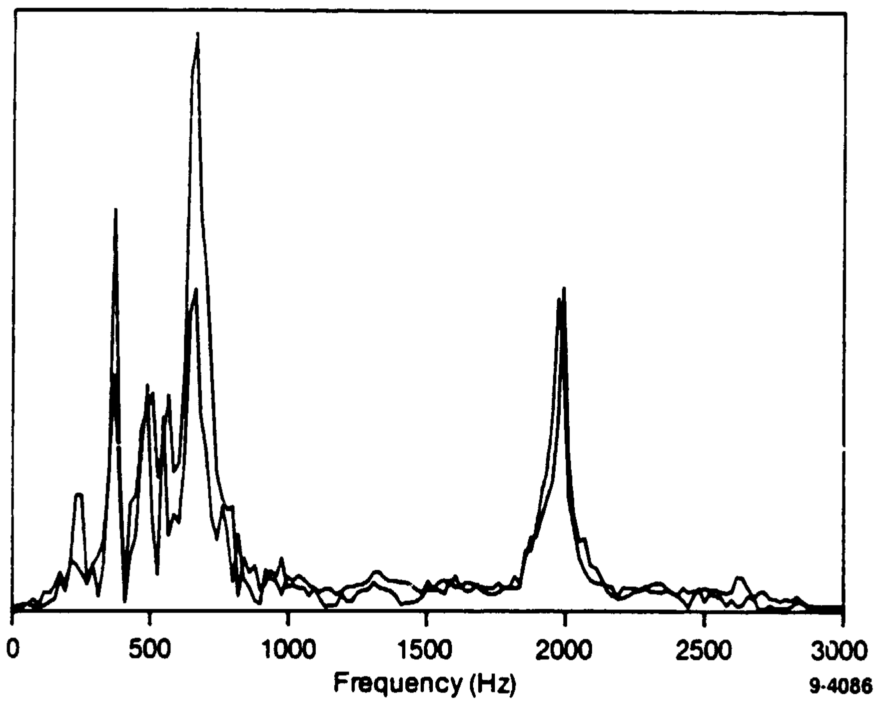

Figure 2. Vacuum chuck repeatability test. To evaluate the repeatability of the vacuum chuck mount, data were collected from Tile 8122 on two occasions, three weeks apart.

Tile Bond Analysis

The central thesis of this work is that bond condition can be determined by studying the vibrational response of a tile excited by acoustical energy. The vibrational modes of a TPS tile can be of either the rigid body type or the flexural type. In rigid body modes, vibration results from rocking, piston, or twisting actions of the rigid tile against the spring action of the SIP. Twisting motions will not be considered here because the displacement sensors used for this work only detect motion normal to the tile surface. In the flexural modes the tile bends as it vibrates; tile stiffness provides most of the spring action. For TPS tiles examined so far, the frequencies of the two types of vibrational modes fortuitously separate into distinct nonoverlapping ranges - the rigid body modes appear below 1400 Hz, while the flexural modes appear above 1600 Hz. This separation aids in the interpretation of some of the phenomena observed in tile vibrational response.

Investigations have centered on identifying response characteristics that reliably predict unbonds. The results discussed below were primarily

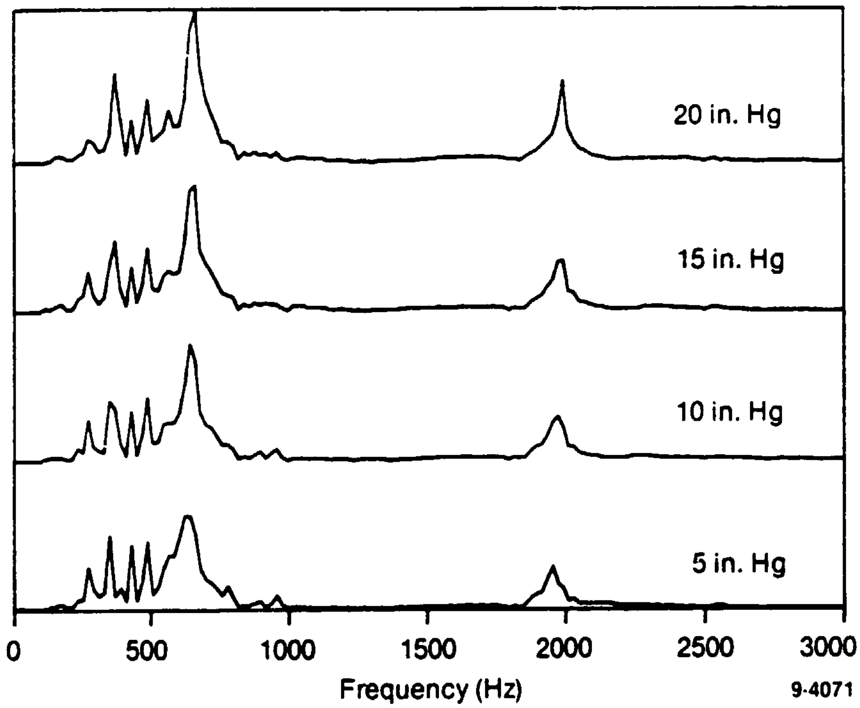

a.

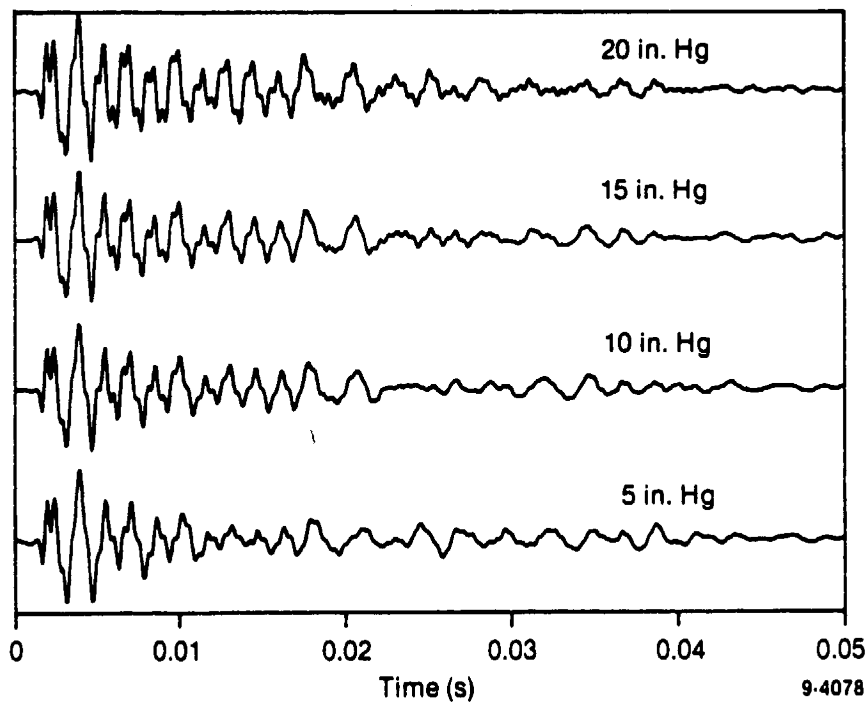

b.

Figure 3. Frequency (a) and time domain (b) responses for four vacuum readings at the vacuum chuck.

obtained with the pedigree tiles, using the vacuum chuck to simulate unbonds. A number of characteristics have emerged as promising unbond indicators. They are listed here and explained in the text which follows:

1. Downward frequency shift of rigid body modes.

2. Amplitude of the vibrational response.

3. Elongation of initial oscillations in transient tile response.

4. Asymmetrical response characteristics in unbonaed tiles.

Downward Frequency Shift of Rigid Body Modes

It was discovered early in this work that unbonds induce downward shifts in the resonance frequencies of some rigid body modes. The spectrum displayed in Figure 4 illustrates this shift. In the case of the 47% unbond, the overall shift to lower frequencies of the rigid body resonance modes is fairly obvious. Lacking a quantifiable measure, the shift is not as obvious for the 20% unbond. Two facts are evident in Figure 4: not all resonance peaks shift the same amount, and amplitudes of the peaks are affected by unbonding. The complicated structure of the spectra sometimes makes it difficult to determine the overall frequency shift. Efforts to develop quantifiable measures of frequency shifts in the rigid body modes were undertaken to remove some of the uncertainties associated with this unbond indicator.

In order to quantify the frequency shifts as unbonding progresses, a measure of the center frequency for each unbond condition is needed. Four measures of the center frequency of the rigid body modes were developed and evaluated. All operate on spectra over the rigid body frequency range of 0 to 1400 Hz. Spectra are calculated using fast Fourier transform (FFT) without windowing. The magnitude of the FFT terms is used in two of the center frequency calculation methods; magnitude squared is used in the remaining two. The four methods of calculating center frequency are as follows:

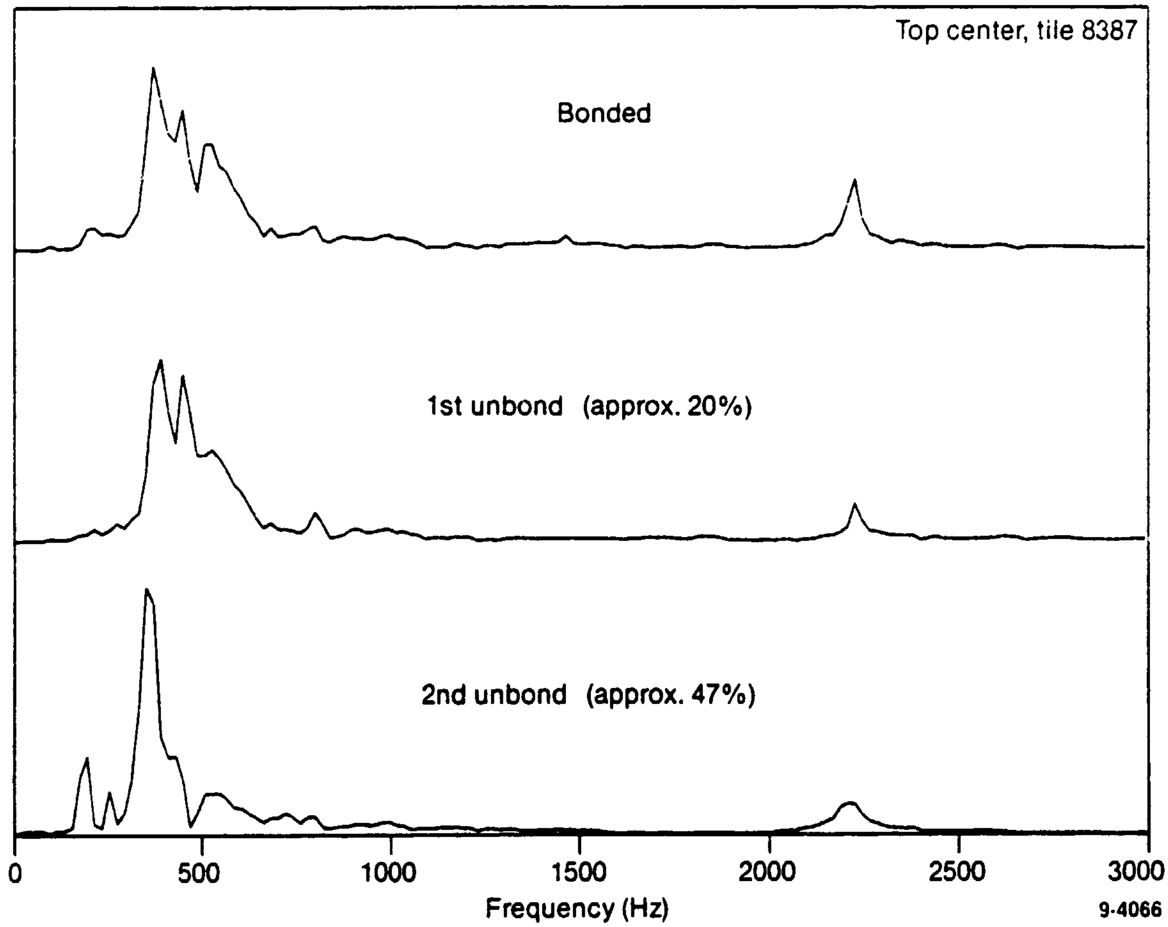

Figure 4. Downward frequency shifts as unbonding increases.

Median Frequency I. The area under the spectrum to the left of the median frequency is equal to the area under the spectrum to the right. Magnitude of the FFT terms is used for spectral amplitude.

Amplitude Moment I. This method is defined by the following equation:

$$f_c = \int fA(f)\, df$$

where

f is frequency,

$A(f)$ is spectral amplitude, and

f_c is the calculated center frequency.

The magnitude of the FFT terms is used for the spectral amplitude.

Median Frequency II. Same as Median Frequency I except squared magnitude of the FFT terms is used.

Amplitude Moment II. Same as Amplitude Moment I except squared magnitude of the FFT terms is used.

The four methods are similar and might be expected to yield similar results. The fact that they do indeed predict unbonds in a consistent manner suggests a robustness to the general approach. The performance of all four methods is described in some detail in the following.

The methods were evaluated by applying them to data collected during unbonding experiments with the three pedigree tiles: 9073, 9074, and 9075. The vacuum chuck was used to simulate unbonds. Data were collected from the three tiles under four bond conditions: fully bonded, 25% unbonded, 50% unbonded, and 100% unbonded (backshop measurement). The 25% unbond was a 2-1/2-in. square region in the upper right corner of the 5-in. square SIP. The entire top half of the SIP was unbonded in the 50% unbond tests. The 100% unbond data was collected while the tile was lying face-up on the optical table; this is also referred to as a backshop measurement. Filler bar was present for all measurements, except of course for the 100% unbond case. Data were collected at three points on each tile, top center, center, and lower center, as illustrated in Figure 5. The spectra collected and the center frequencies calculated by the four methods for tile 9073 are presented in Figures 6 through 8. Similar data were collected from the other two pedigree tiles. Results from the three tiles are summarized in Figures 9 through 11.

The four measures of center frequency are in substantial agreement. For top center and center point data, all four methods indicate a shift to lower frequencies with increased unbonding. For lower center point data the four methods are likewise in agreement, although the shift to lower frequencies with unbonding is not indicated. The Amplitude Moment I method displays the least tile-to-tile variance, which may indicate better noise tolerance.

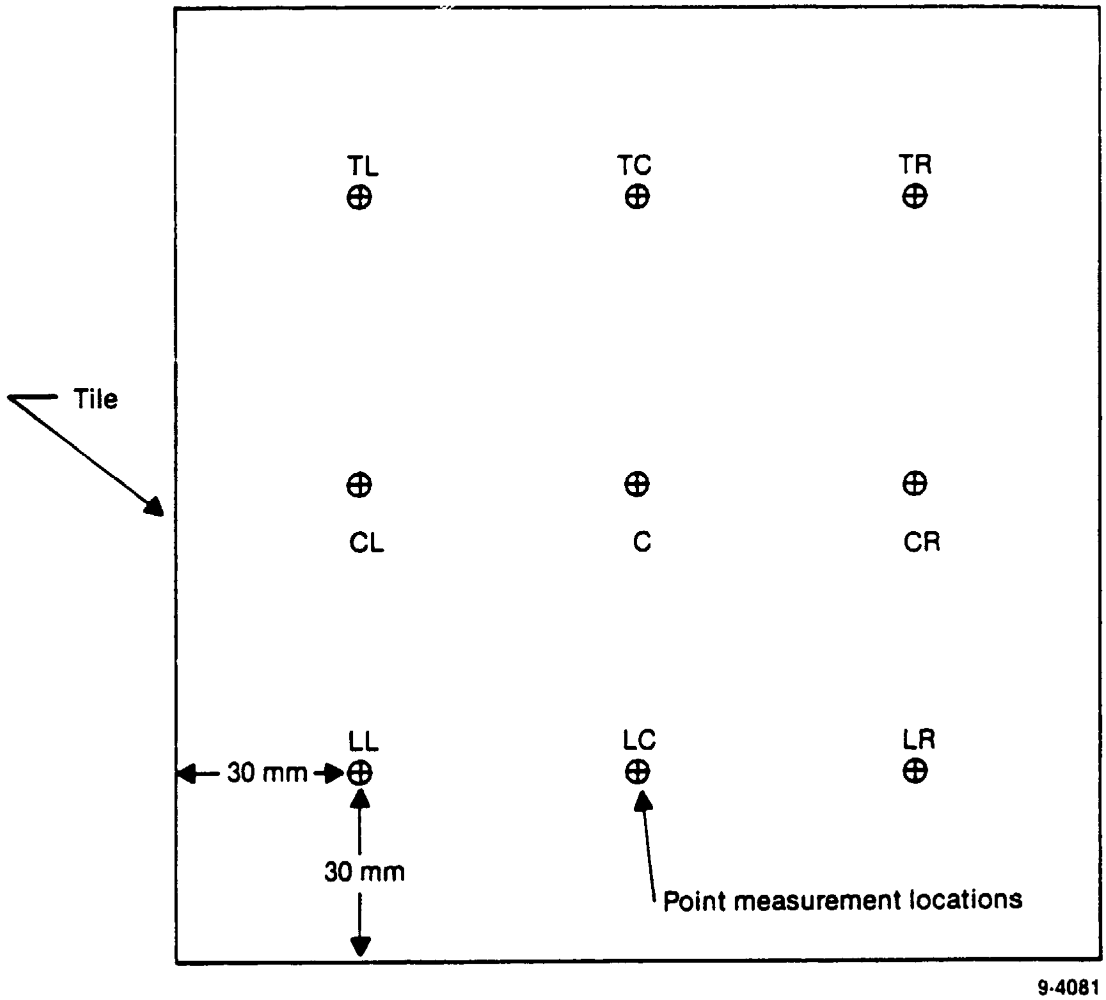

Figure 5. Vibration measurement points.

The shift in the center frequency for the rigid body modes appears to be a reliable unbond indicator when the sample point is over or close to the unbond region. When the sample point is on the opposite side of the tile from the unbond region, the shift seems absent. The reason for this behavior has not been thoroughly investigated, although an explanation has been hypothesized. The shifts observed at the top center and center points can be reasonably explained by considering the tile to behave as a mass on a spring, the SIP being the spring. As the tile is unbonded, the spring is weakened. Since the natural frequency of a mass-spring system is proportional to the square root of the spring constant, weakening the spring lowers the frequency of the vibration. The explanation for the seemingly anomalous behavior at the lower center point is thought to have something to do with the migration of rocking mode nodes. A rocking mode node can be thought of as the fulcrum

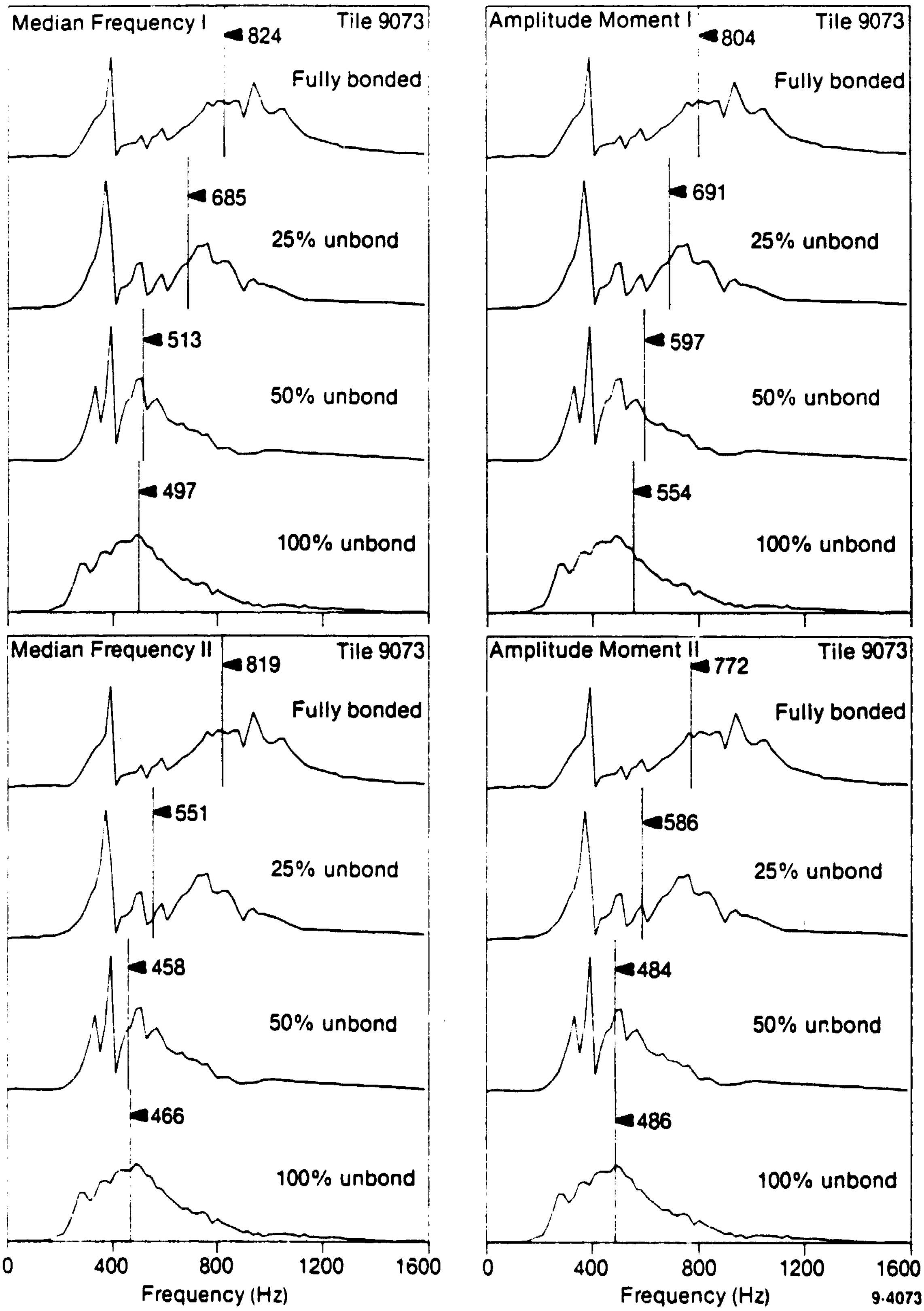

Figure 6. Four methods of calculating center frequency applied to data collected from the top center point of tile 9073.

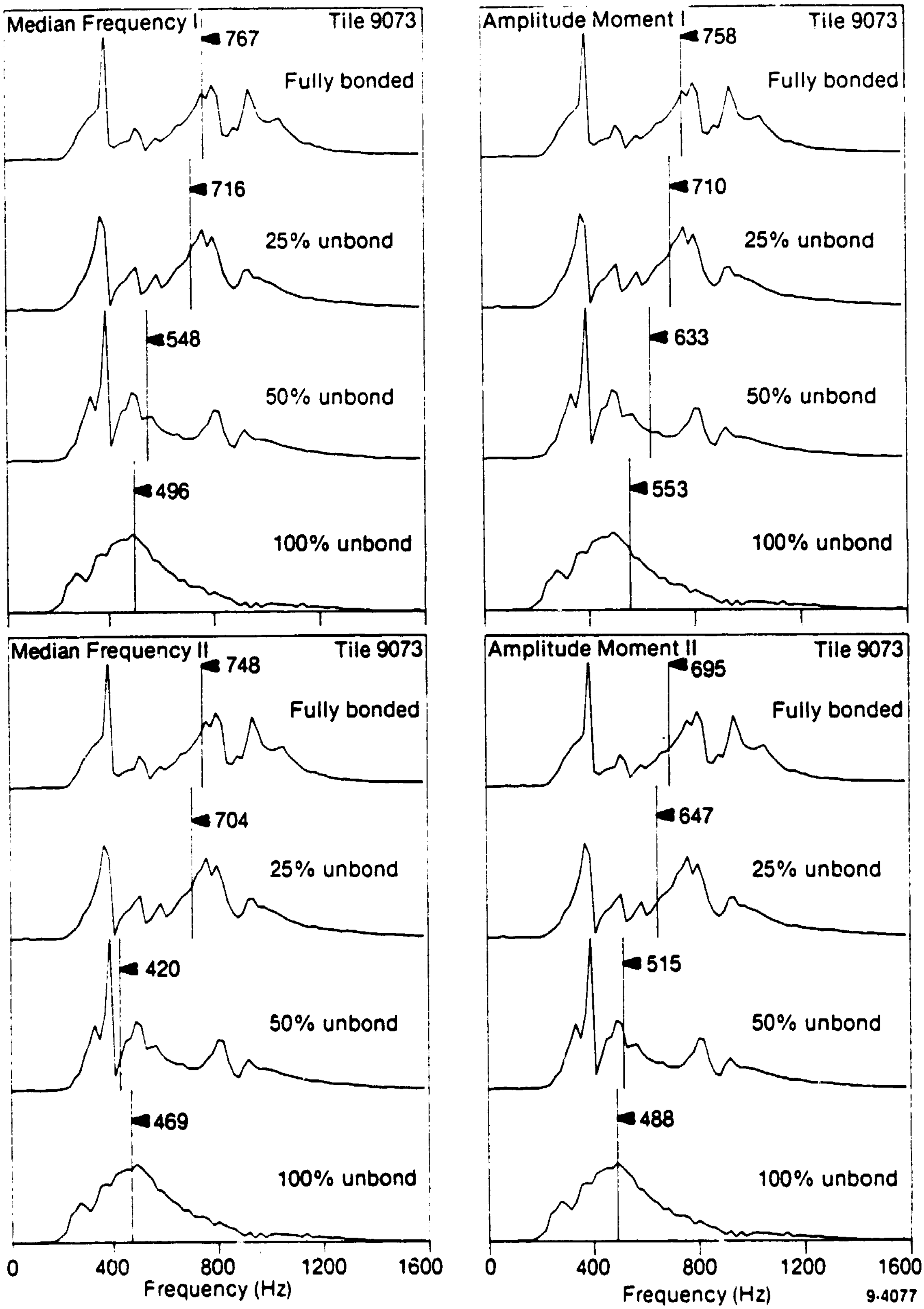

Figure 7. Four methods of calculating center frequency applied to data collected from the center point of tile 9073.

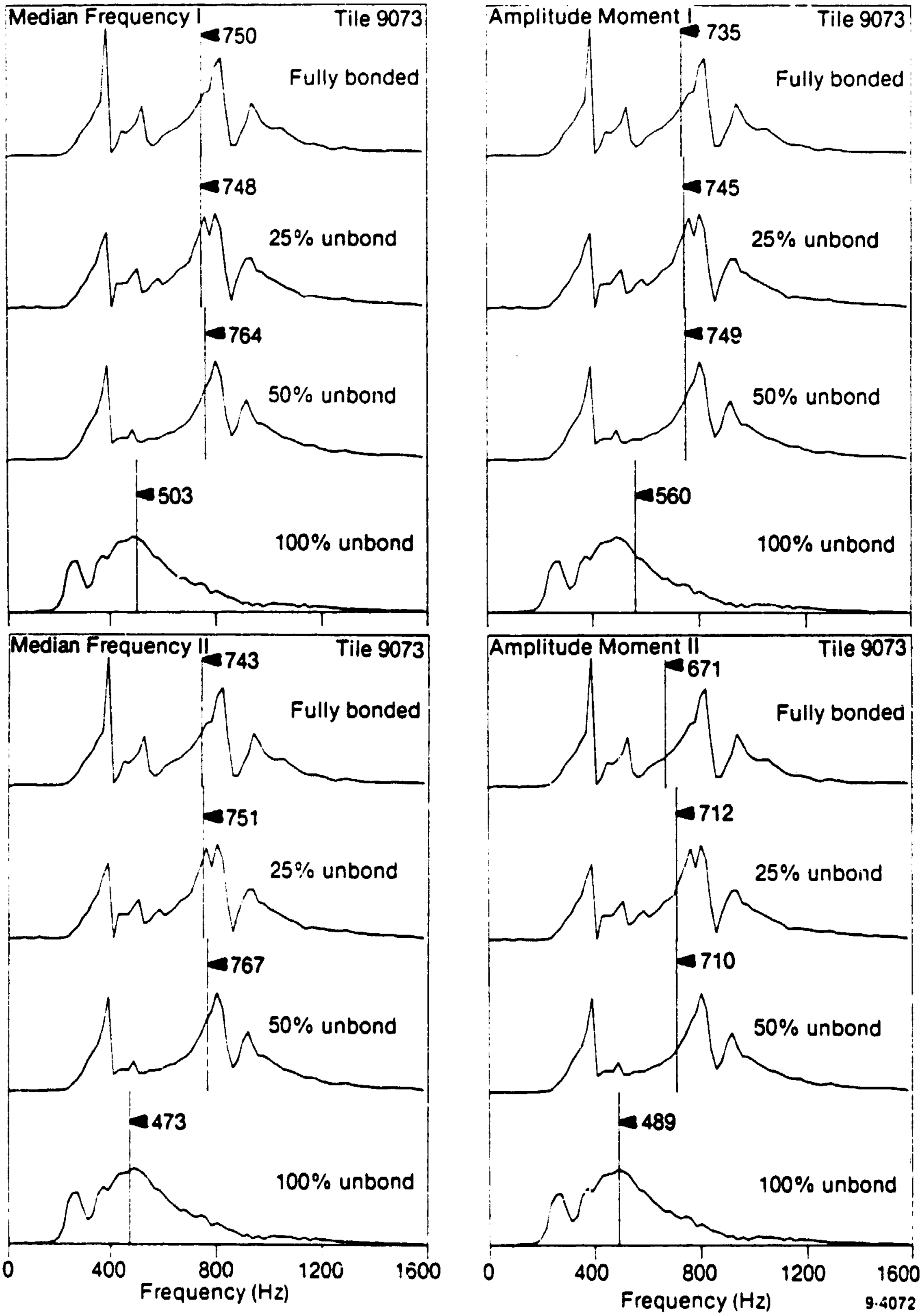

Figure 8. Four methods of calculating center frequency applied to data collected from the lower center point of tile 9073.

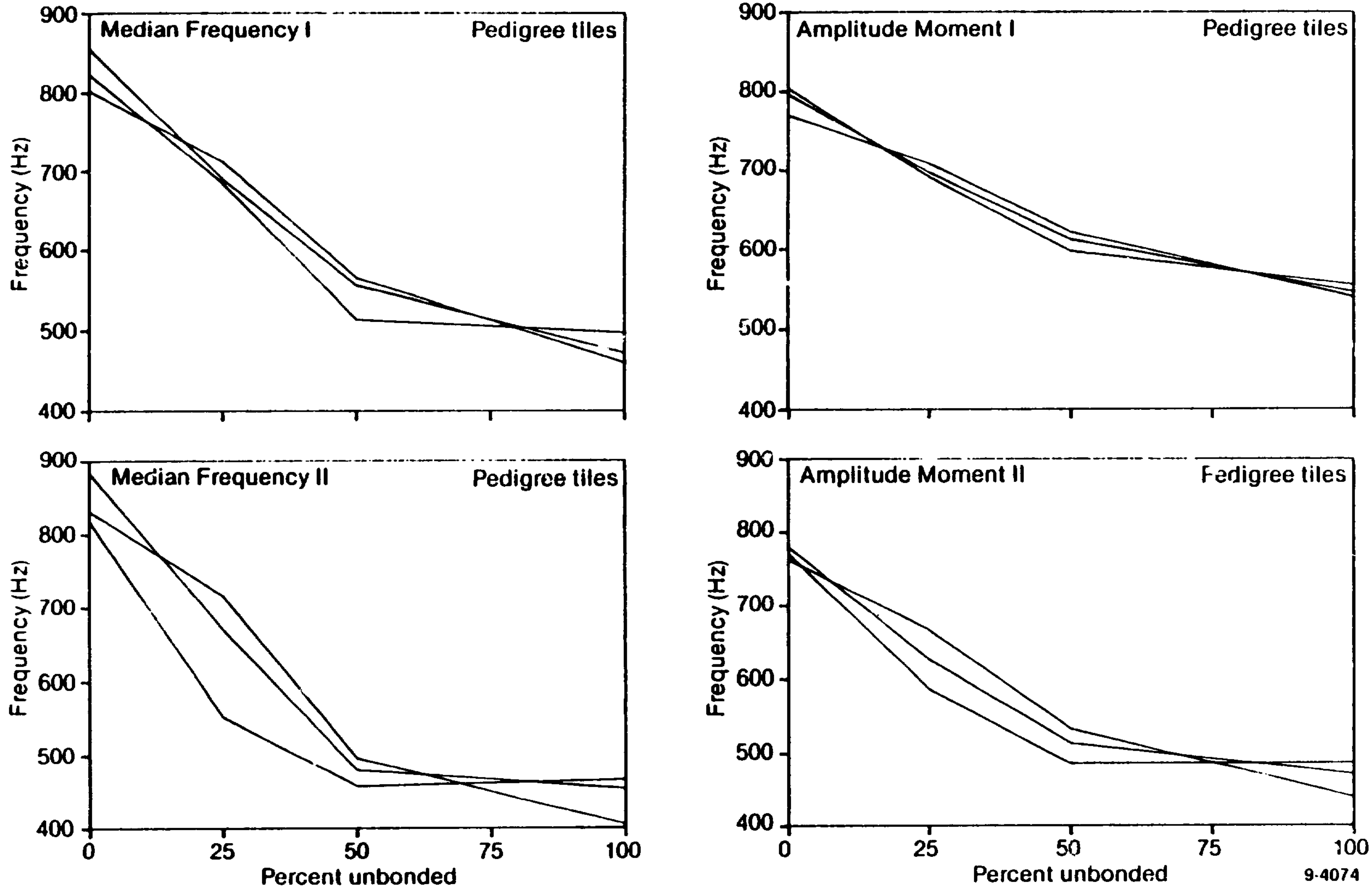

Figure 9. Calculated center frequency as a function of percent unbond for the top center point of the three pedigree tiles. The results of four different methods are shown.

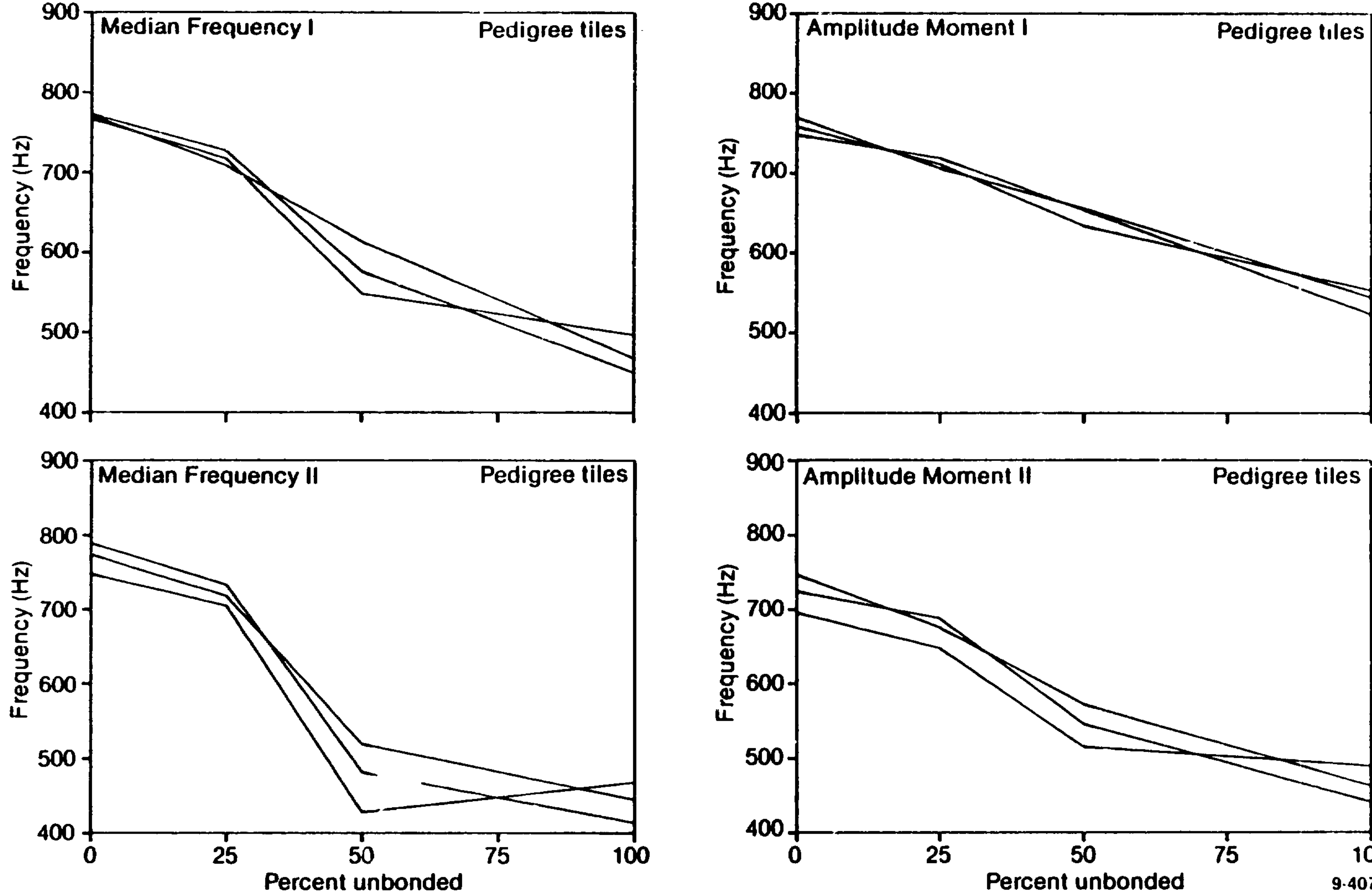

Figure 10. Calculated center frequency as a function of percent unbond for the center point of the three pedigree tiles. The results of four different methods are shown.

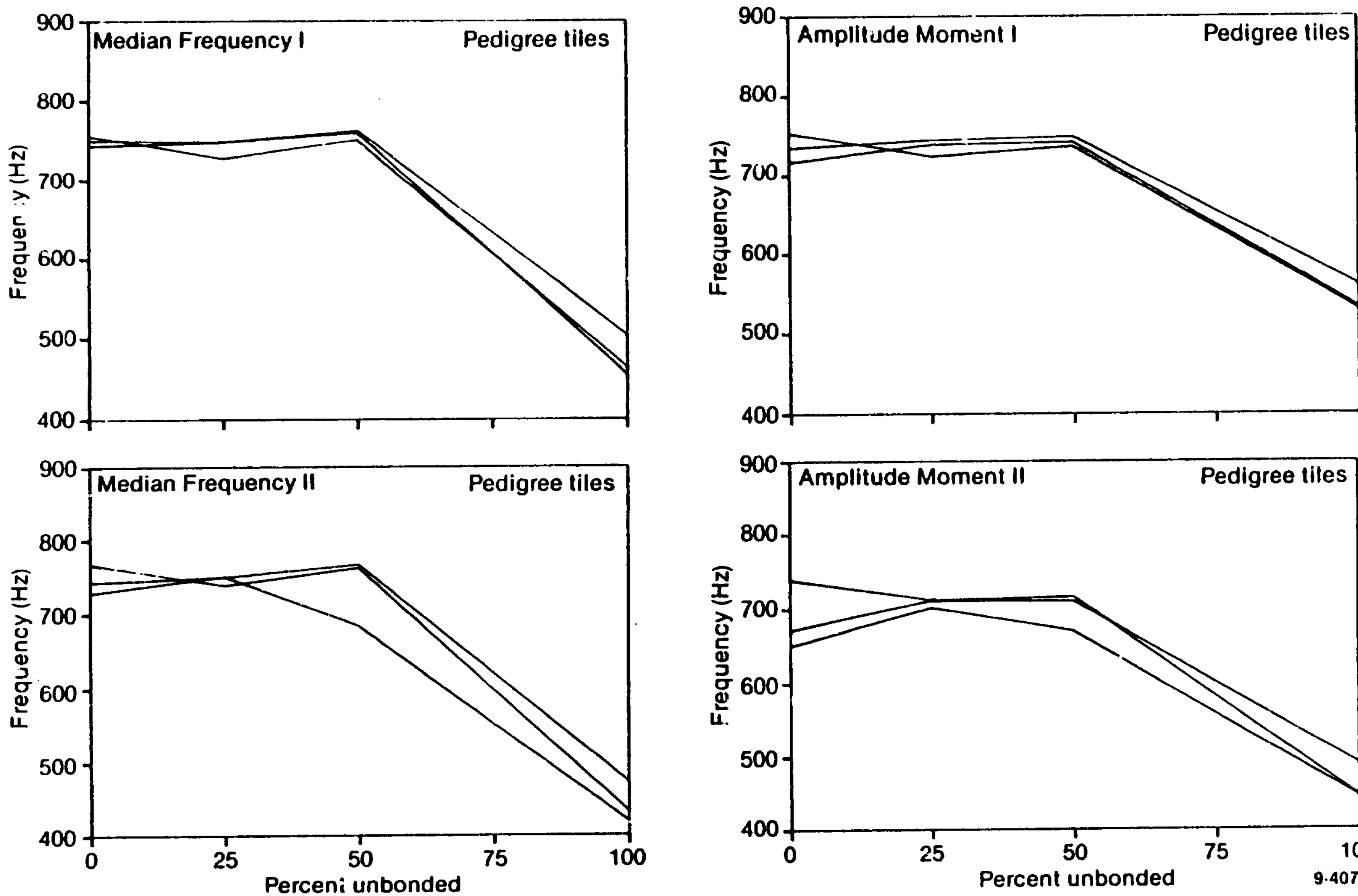

Figure 11. Calculated center frequency as a function of percent unbond for the lower center point of the three pedigree tiles. The results of four different methods are shown.

about which a tile rocks. The measured amplitude of a rocking mode will be affected by the proximity of the sample point to the fulcrum. The amplitude at points near the fulcrum will be less than at points far from the fulcrum. Points on the fulcrum will have zero amplitude, and that particular rocking mode will go undetected. As the top region of a tile is unbonded, it is thought that some of the rocking mode nodes migrate downward, away from the unbonded region, deeper into the bonded region. Considering the tile to be a rigid body connected to a bed of springs, unbonding amounts to removing springs in a region. As unbonding progresses, the fulcrum about which the tile rocks migrates toward the center of the region of remaining springs. As the fulcrum moves closer to a sample point in the bonded region, the associated rocking mode will contribute less to the overall motion of the vibrating tile. Hence, the frequency shift affecting this mode will be less detectable. Other modes and other affects will then dominate the tile vibrational response.

The explanations presented above could be verified if nodes could be tracked during unbonding experiments. This has proven difficult to do using speckle interferometry (SI), the standard technique for visualizing nodes. The difficulty stems from the fact that a single rigid body mode can usually not be excited by itself. Rigid body resonance modes overlap because they tend to be broad (due to damping), closely spaced, and coupled by frictional forces. The sinusoidal tone used in SI usually excites multiple rigid body resonance modes, making visualization of individual nodes difficult or impossible.

Interest in node tracking transcends the desire to explain observed frequency shifts. Knowledge of the behavior of individual resonance modes, especially those most affected by unbonding, would be invaluable for evaluating bond condition. Unbond indicators resulting from such an understanding of mode behavior would probably be more useful than the largely empirical indicators identified so far; supported by a better understanding of the physical phenomena, they would probably be more predictable and accurate. It is hoped that modal analysis techniques, employing point sensor data, will provide information necessary to understand the behavior of individual resonance modes.

Center frequency (as defined above) shows promise of being a reliable unbond indicator when the sample point is near an unbond. To use center frequency for unbond determination, the "good" center frequency must be known beforehand. It may be possible to determine this from knowledge of tile geometry, unless center frequency is very sensitive to minor variations in geometry or to random variations introduced during mounting. If it is sensitive, center frequency may still be used for bond analysis, but it would require an empirical determination of the "good" value after mounting. The technique would not then be useful for inspecting initial tile installations. Rather it would be used for postflight examinations. Results obtained from the pedigree tiles suggest that "good" center frequencies may be accurately predicted from nominal geometries. More study of center frequency and the factors that affect it is required.

The measured dynamic response of a tile with an unbond depends on the relative locations of sample point and unbond. As previously stated, the frequency shift of the rigid body modes is obvious only when the sample point is in the proximity of the unbond. This is not necessarily a bad situation. As will be discussed later, asymmetrical behavior of an unbonded tile could be the footprint used to detect the unbond.

Amplitude of the Vibrational Response

Larger vibrational amplitudes have been found to correlate with unbonds. Figure 12 shows time series data collected from tile 9074. A relationship between amplitude and the presence of an unbond is evident. However, as illustrated in Figure 13, amplitude also depends on the relative locations of unbond and sample point. The sample point is the same for all five plots in Figure 13, the lower right corner. The speaker position is also the same for all five plots, to the left of the tile. The peak-to-peak amplitude is largest when the unbond is across the bottom. When this is the case, the sample point is over the unbond, and the peak-to-peak amplitude is double the amplitude of the fully bonded tile. When the unbond is along the right side, the sample point is also over the unbond, but the increase in amplitude is only 36%. When the sample point is not over the unbond, the increase is absent or less evident.

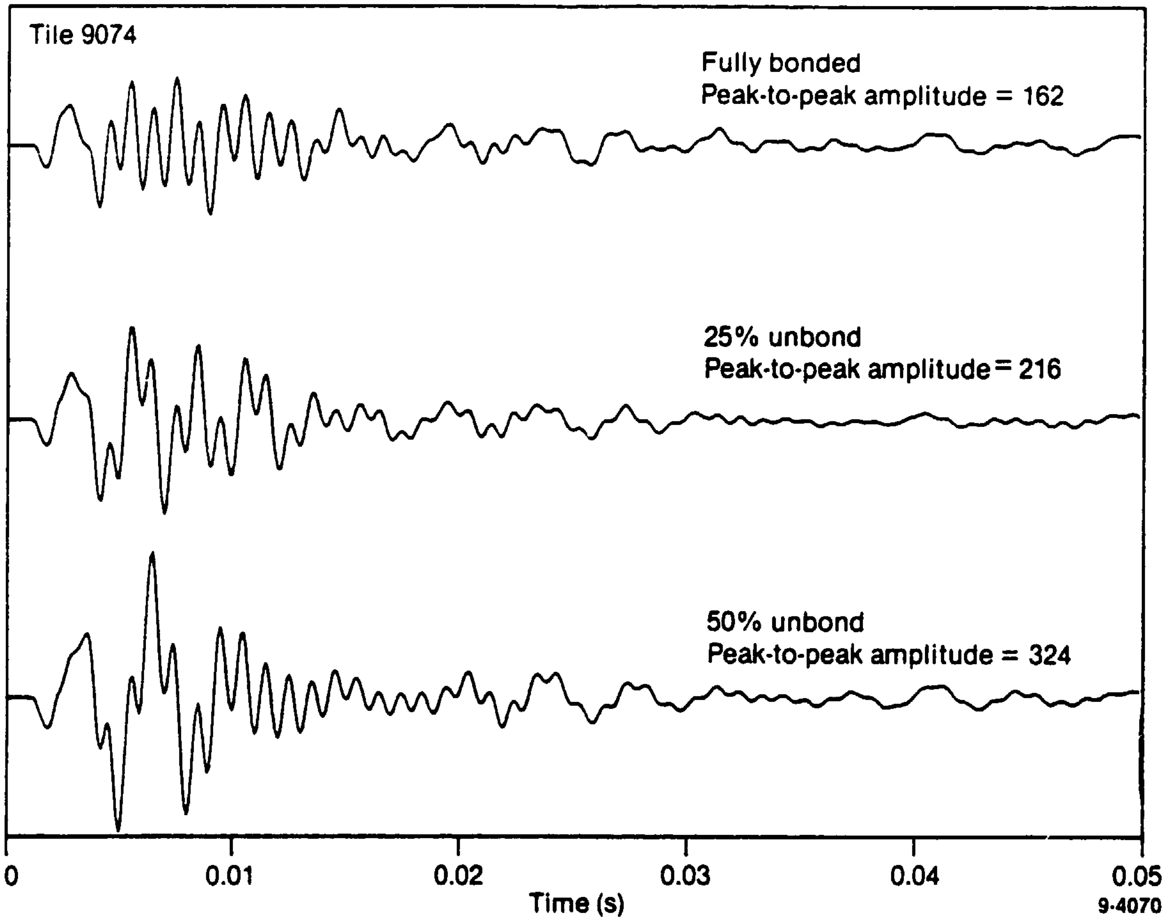

Figure 12. Effects of unbond on amplitude.

The amplitude data discussed here were not collected with the point sensor developed for this work. That sensor has some outstanding characteristics, but providing measurements of absolute amplitude is not one of them. The problem stems from the fact that measurements are proportional to brightness of reflected light as well as displacement. The reflectivity of tiles varies from point-to-point, thereby precluding comparison of amplitude data from two different points on a tile. Amplitude data were collected with a laser vibrometer that required the attachment of a mirror to the tile. The vibrometer is not considered fieldable because of the mirror requirement. A new or modified sensor would be necessary if amplitude is to be used as an unbond indicator. The existing sensor could be used if it were possible to calibrate it at each sample point, and a fairly simple method of calibrating the current sensor using a dither signal has been proposed. If amplitude is determined to be a necessary measurement for unbond detection it is felt that an appropriate sensor could be developed with existing technology.

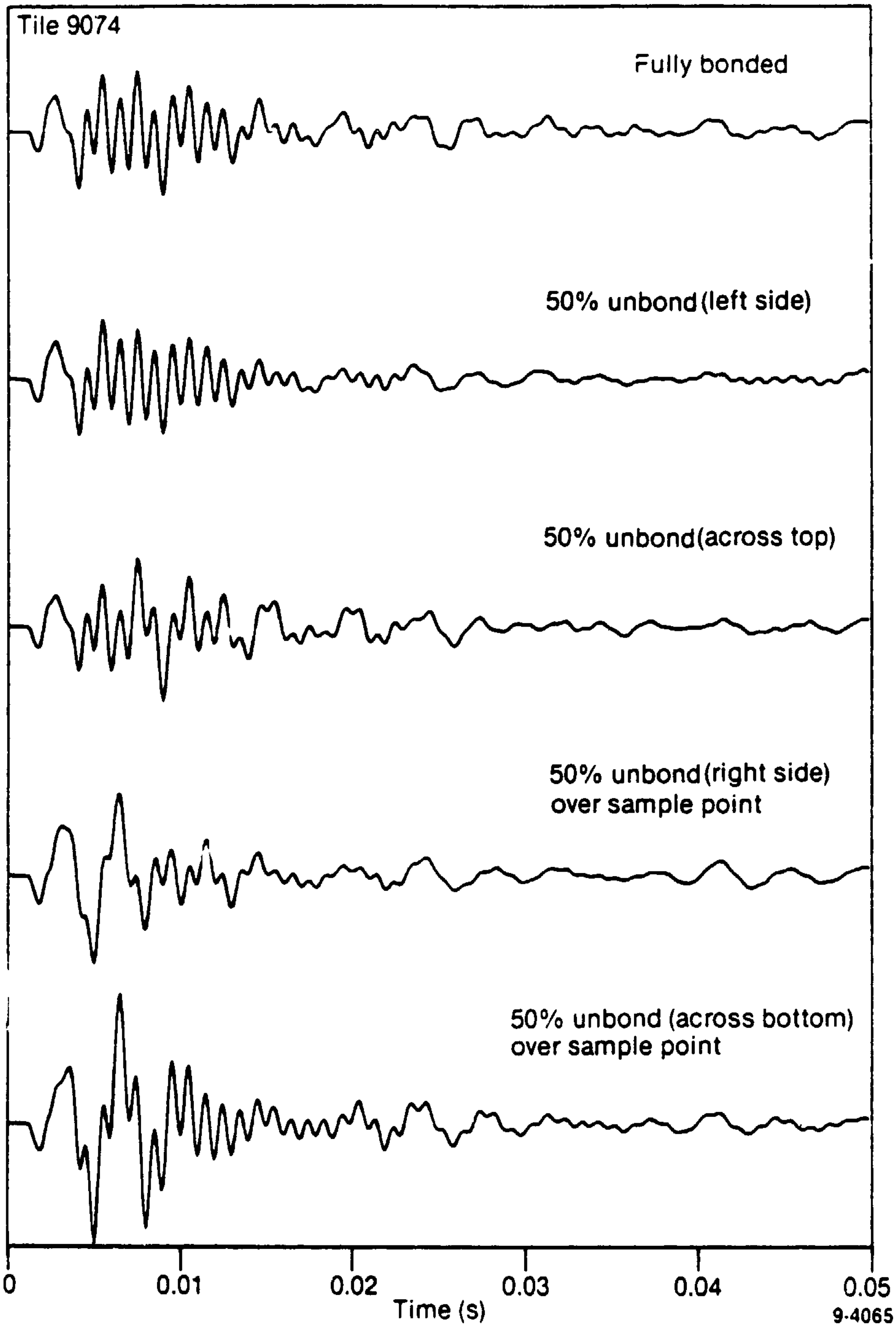

Figure 13. Effects of location of unbond on amplitude.

Elongation of Initial Oscillations in Transient Tile Response

The first few milliseconds of tile vibration following excitation exhibit a characteristic that predicts unbonds in the pedigree tiles. This characteristic is the duration of the first few oscillations in the time series data. Figure 14 shows the first three milliseconds of time series data for three bond conditions. As unbonding increases an elongation of the oscillations occurs and the time between zero crossings increases. This phenomenon may be the time domain equivalent of the downward frequency shifts observed in the rigid body modes. If so, there may be little to gain in studying both phenomena because the bond condition information contained in one may be duplicated in the other. On the other hand, the two may not be that closely related. The time domain phenomenon may provide information about resonance modes not observable in spectra estimated using fast Fourier transform techniques since they necessarily represent time averages of the

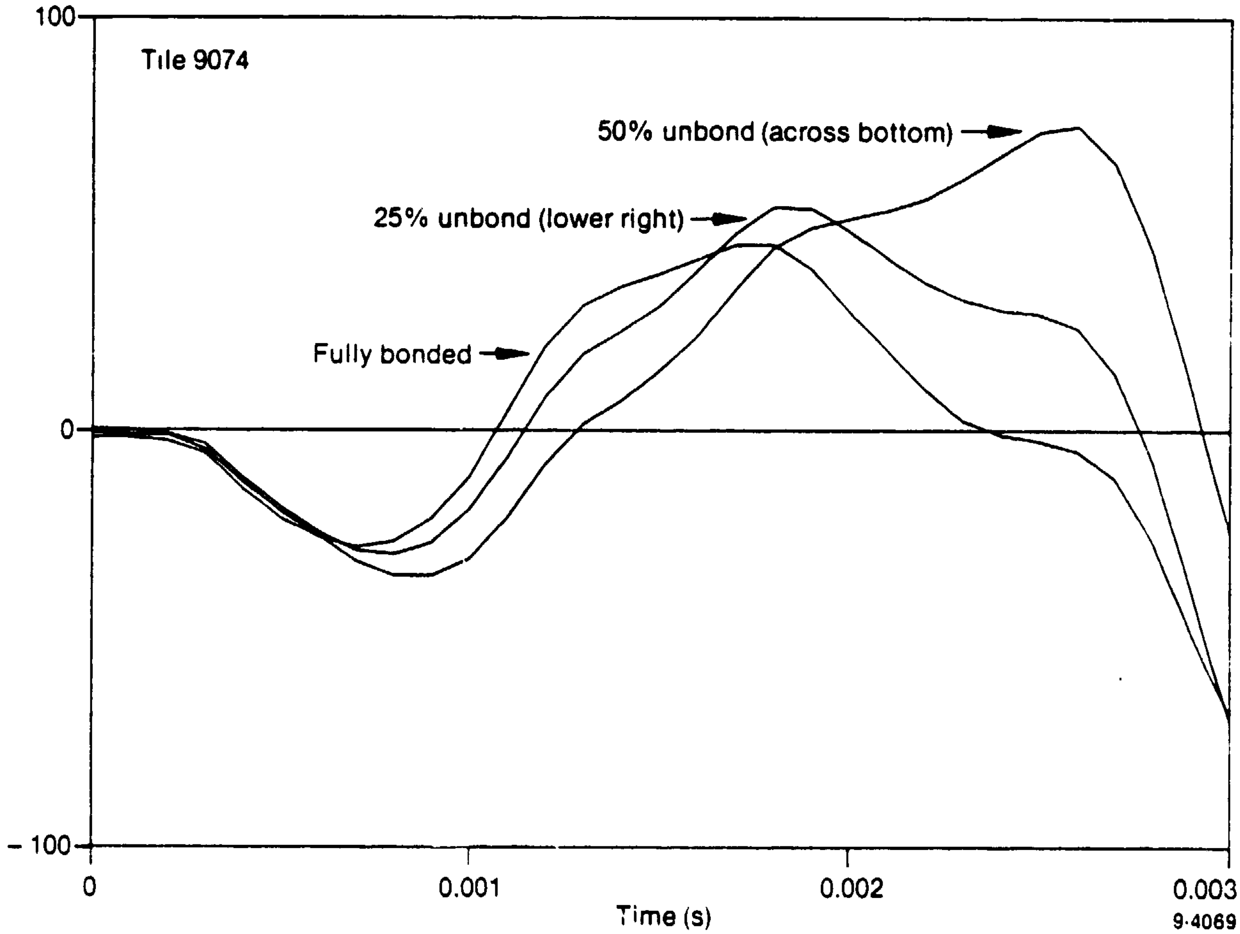

Figure 14. Effects of unbond on initial oscillations.

frequency content of a signal. The frequency content of a transient process such as tile dynamic response changes with time (the process is nonstationary). A time average may not represent the frequency content at a particular time well, especially if dominant resonance modes at that time are rapidly decaying. Hence, there is reason to continue consideration of this time domain unbond indicator.

Unbond effects on initial oscillations are affected by the relative locations of sample point and unbond. Elongation of initial oscillations diminishes as the distance between sample point and unbond increases. Evidence suggests that the relative positions of speaker and unbond may also be significant. This is very similar to the behavior of unbond indicators already discussed. The data from unbonded tiles plotted in Figure 14 were collected at points over the unbonds.

Asymmetrical Response Characteristics in Unbonded Tiles

The tile response characteristics discussed above exhibit a dependence on the relative locations of sample point, unbond, and speaker. This behavior suggests that an asymmetrical response may be useful for identifying unbonds. Asymmetrical behavior of an unbonded tile is illustrated in Figures 15 and 16. The top two plots in Figure 15 show the response of a bonded tile at two measurement point locations, top left and top right. The bottom two plots show the response of an unbonded tile at the same two measurement locations. Speaker position is the same for all these plots and the location of the unbond is the same. It is apparent that the differences in top right and top left spectra are greater when an unbond is present.

Figure 16 shows the effects of varying the speaker position. The top two plots show the effect on a bonded tile of moving the speaker from side to side while keeping the measurement point location fixed. The bottom two plots show the effect on an unbonded tile (same unbond location). The spectrum at a given point is apparently more sensitive to changes in speaker location when an unbond is present.

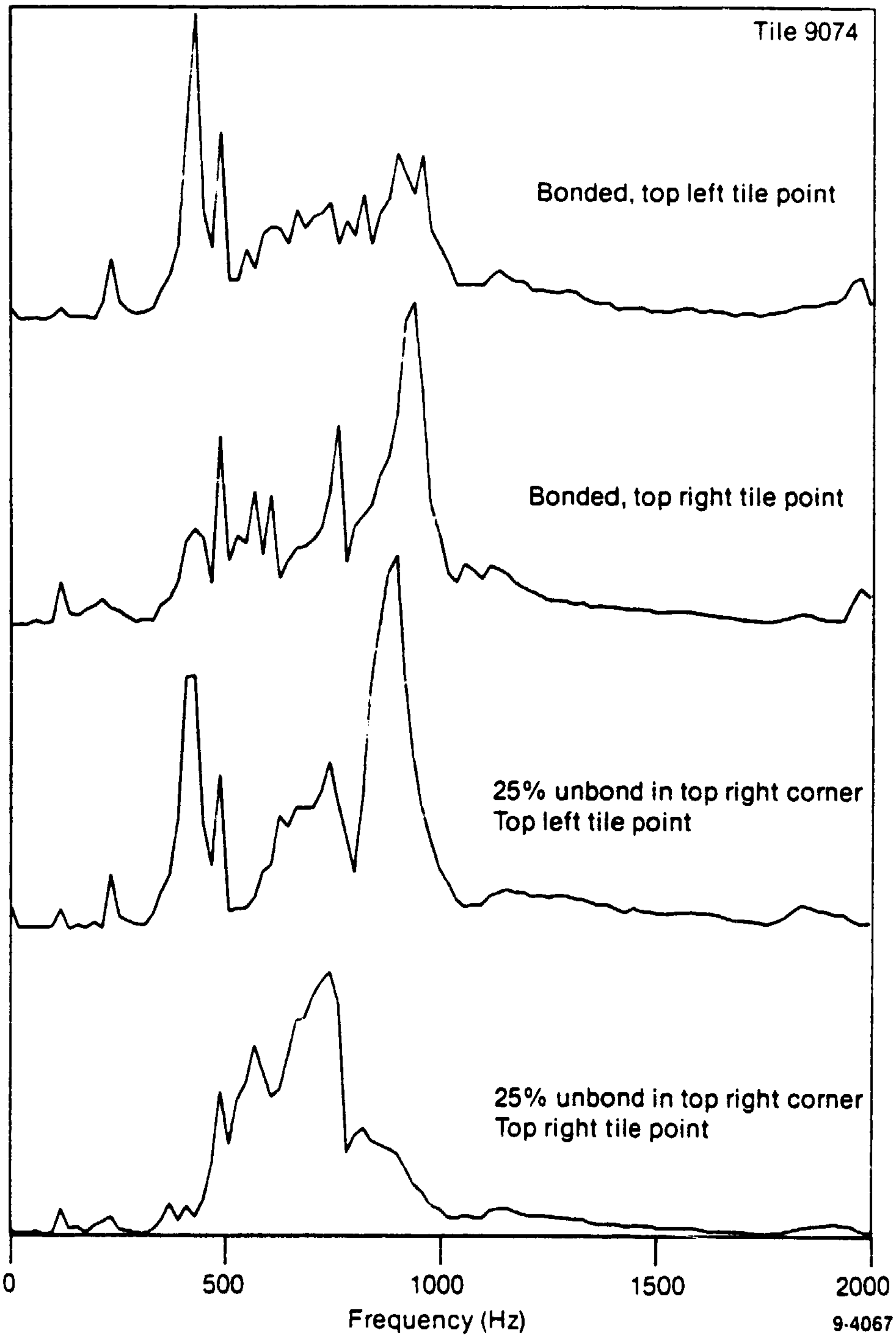

Figure 15. Effects of sample point location.

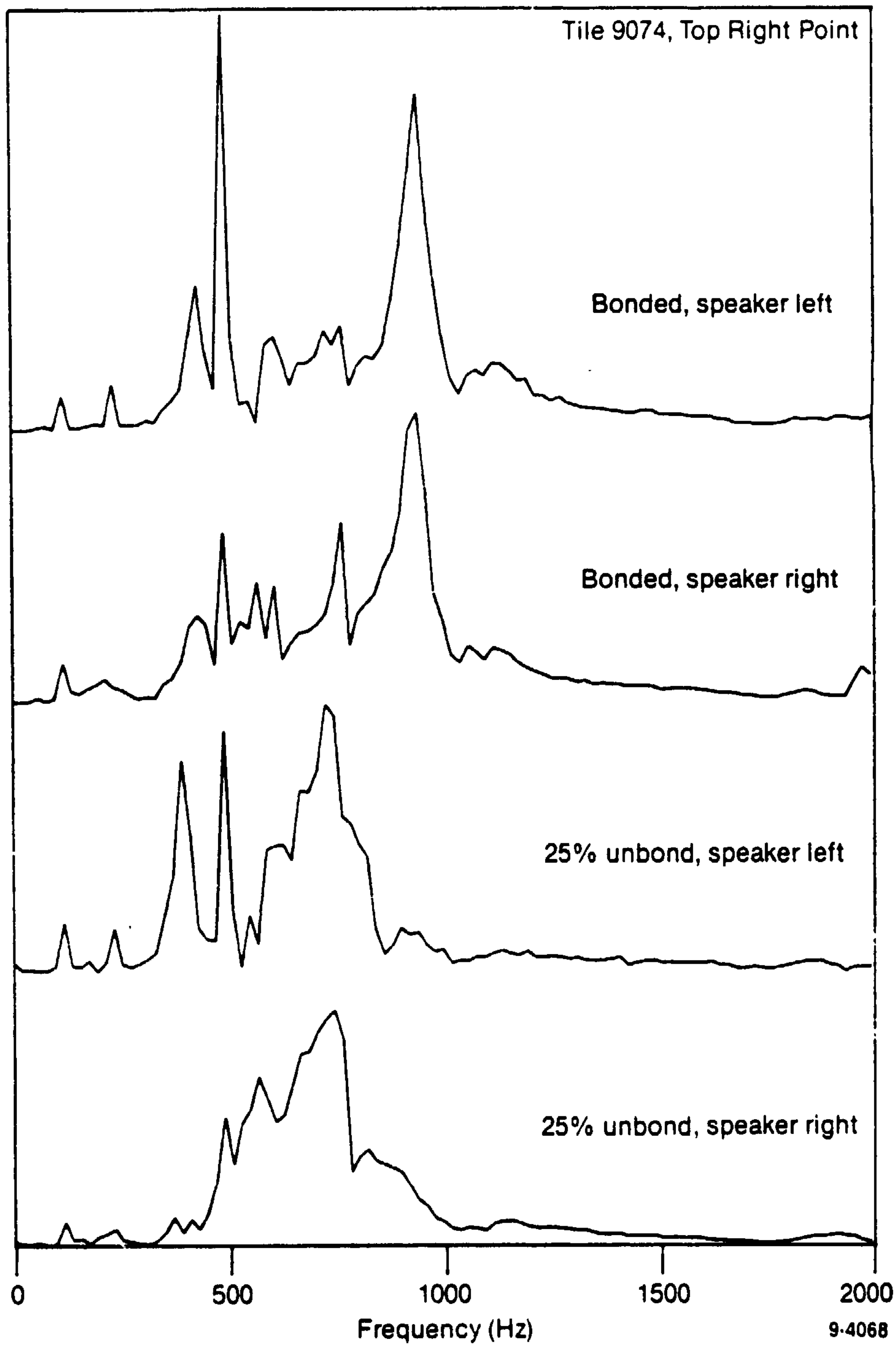

Figure 16. Speaker position effects, tile 9074, top right point.

This unbond indicator is particularly attractive since it does not require prior assumptions about "good" tile behavior. It is based on the following two premises:

1. An asymmetrical bond results in asymmetrical tile dynamic response characteristics.

2. Asymmetrical behavior normally observed in bonded tiles is much smaller than asymmetrical behavior due to significant unbonds.

More work is required to verify these two assumptions, as well as devise a method of quantifying spectral asymmetry. Finally, it is clear that this unbond indicator would not be expected to be effective at detecting symmetrical unbonds.

Filler Bar

Most of the experimental work conducted during Phase I was done on tiles without filler bar. With the development of the vacuum chuck, it became possible to conduct experiments with filler bar. Consequently, most of the results obtained during Phase II include filler bar. Figure 17 shows the effect of filler bar on tile dynamic response. Filler bar seems to have an overall stiffening effect, resulting in upward frequency shifts in both flexural and rigid body modes. The effect of filler bar is significant, thus filler bar must be used to accurately assess tile response.

Glass Coating

The effect of the glass coating on tile dynamic response was investigated. Three identical tiles of LI900 material were prepared, two from the same batch of silica (tiles 9091 and 9092). Tile 9091 received the glass coating, the other two were left uncoated. The response of the three tiles appears in Figure 18. The glass coating has little effect on rigid body modes, which primarily occur below 1400 Hz, but has a significant effect

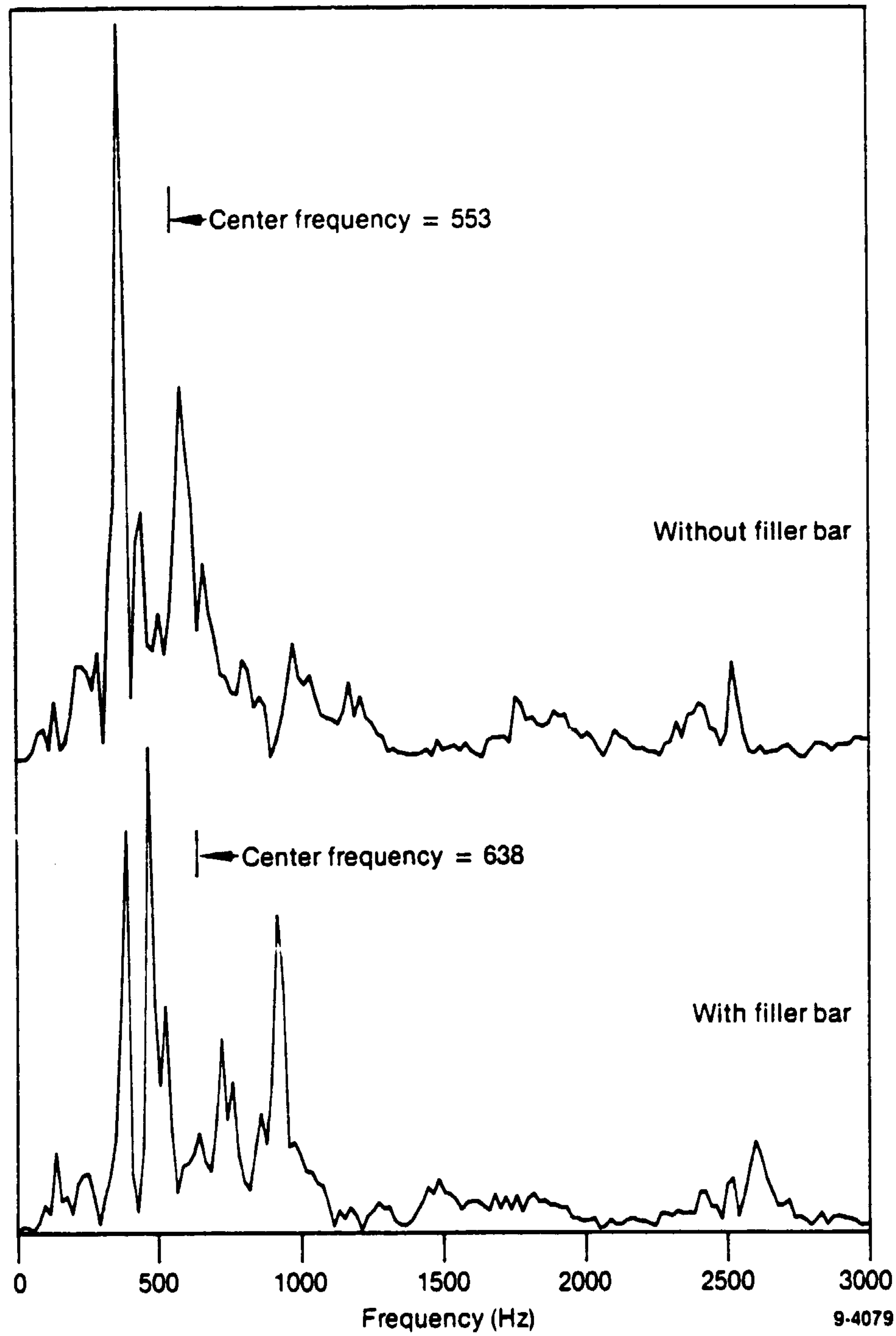

Figure 17. Filler bar effects.

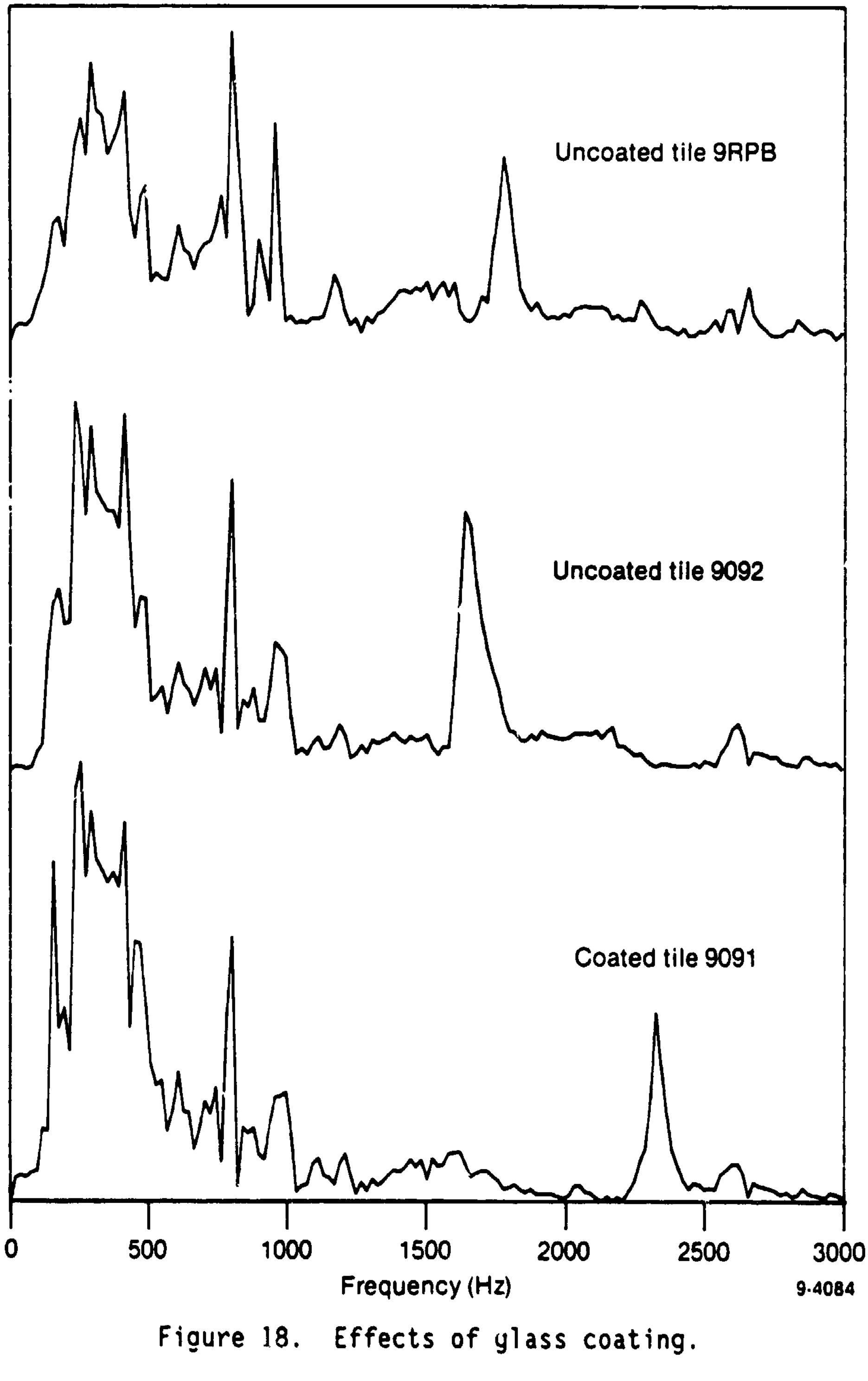

Figure 18. Effects of glass coating.

on flexural modes. In particular, the strongest flexural mode observed in these tiles experiences an upward shift of more than 500 Hz due to the coating. This behavior is consistent with current understanding of the nature of rigid body and flexural vibrational modes. The glass coating stiffens the tile without affecting the characteristics of the SIP. This stiffening would be expected to affect only the flexural modes.

Water Ingress

Preliminary studies were conducted to estimate the sensitivity of the laser point sensor to absorbed water. Tile INL-01 was baked out and bonded to an aluminum plate. Filler bar was not included in this preliminary experiment. Tile response was measured at three points before the introduction of water. Water was injected into the tile at six injection points, identified in Figure 19. Initially, two grams (1% of tile weight) of water was distributed equally between injection holes 1 through 3, and tile dynamic response was measured. This process was repeated for 2 and 5% water content also. Finally, an additional 5% water was distributed between holes 4 through 6, and the dynamic response was measured. In this last experiment total water content was 10%. The results appear in Figure 20. These preliminary results suggest that small quantities of water do not have a significant effect on tile dynamic response. The most notable effect is to the dominant flexural mode around 2500 Hz. The frequency of this mode shifts downward slightly and the amplitude increases somewhat. Further investigations are warranted in this area.

SIP Aging

Preliminary studies were conducted to assess the effects of SIP aging on tile response. This is an important issue since bond verification in the field will have to account for aging phenomena. The aging studies were conducted on tile INL-02. Experiments were designed to be consistent with the fatigue behavior tests reported by P. O. Cooper and J. W. Sawer.[1]

Tile INL-02 with 0.160 in. SIP was bonded to an aluminum plate with filler bar. Tile response was measured before the aging process began. The

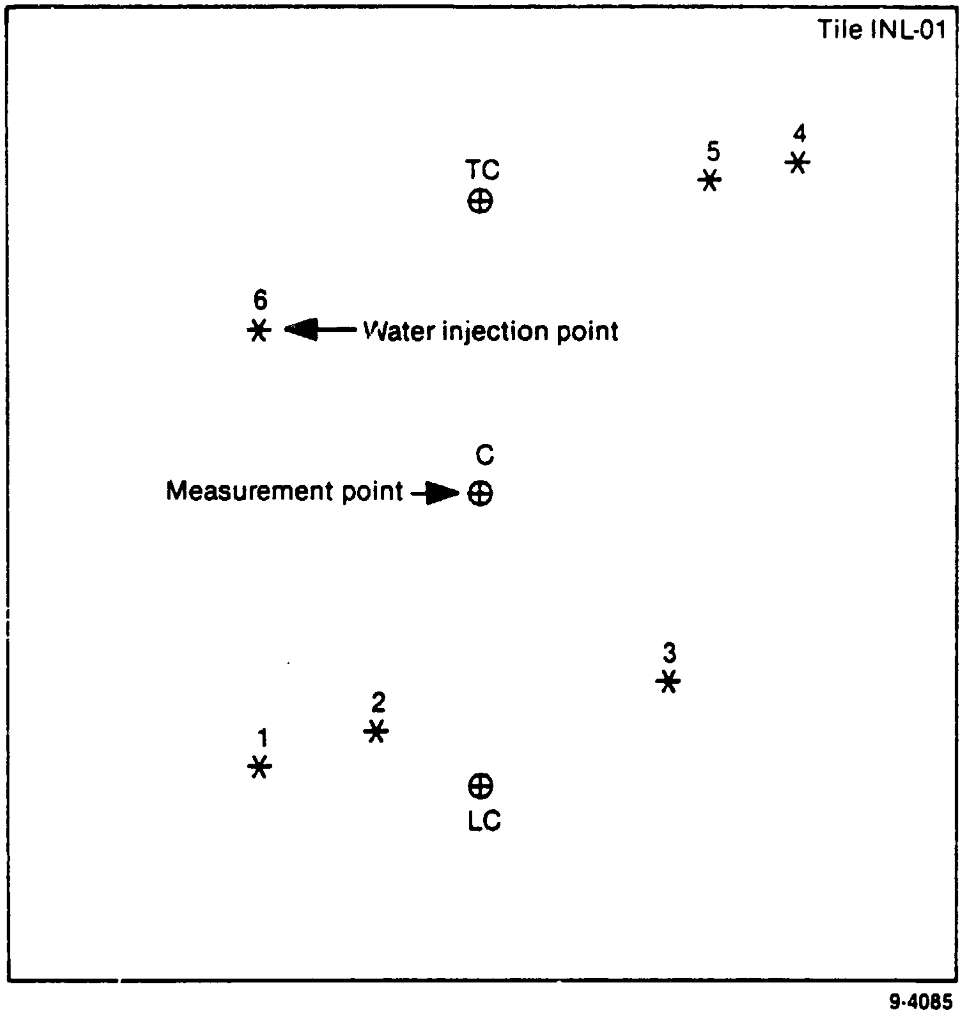

Figure 19. Water injection points.

tile/SIP system was then stressed in an Instron tensile testing machine. The aluminum plate was clamped to a rigid fixture and a vacuum fixture was attached to the face of the tile. A 5 in. diameter O-ring was used to provide a good seal between the vacuum fixture and the tile face. Using this setup, a vacuum of 9.82 psi was obtained between the vacuum fixture and the tile face.

A fully sinusoidal load of 145 lb or 5.8 psi was placed on the tile/SIP system. After the first cycle, a displacement of 0.1 in. was recorded. Forty more cycles were run, and the displacement appeared to remain constant. A cycle of 160 lb or 6.4 psi was attempted, but the seal broke at 149 lb. The dynamic response of the stressed tile was then measured.

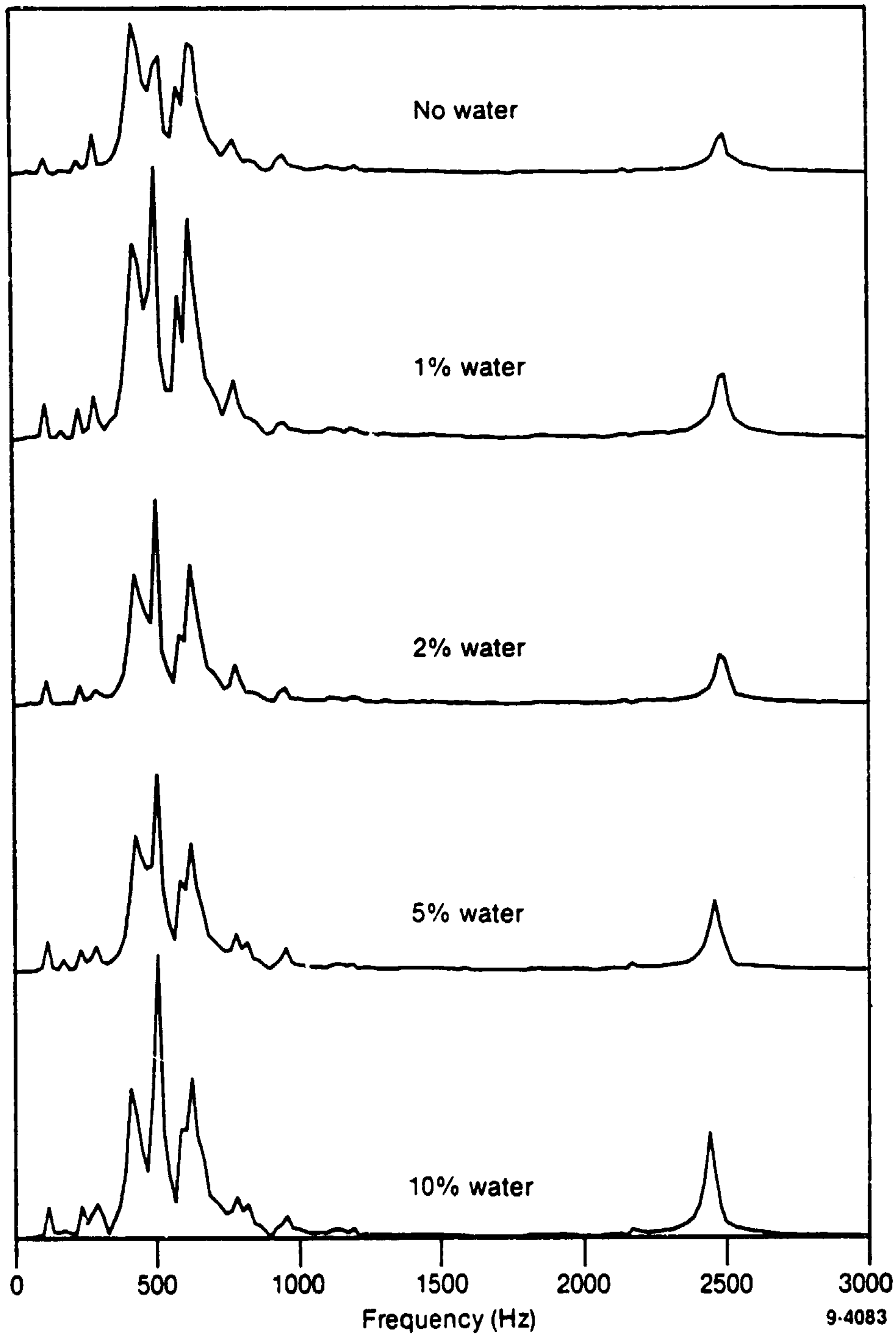

Figure 20. Water ingress test data.

The tile/SIP system was stressed a second time. A soft rubber gasket, 0.5 in. thick, was used this time instead of the hard rubber O-ring. (The O-ring had cracked the glass coating of the tile during the first test and a vacuum could no longer be maintained using it.) With the soft rubber gasket a vacuum of 10.8 was obtained. This allowed the fully sinusoidal loading to reach a maximum of 165 lb or 6.7 psi. The loading was cycled at 3.7 cycles/minute for 75 minutes. This corresponded to 260 cycles. During this time the total displacement (including the stretching of the soft rubber gasket) was a constant 0.15 in.

Results appear in Figure 21. The first two plots in the figure illustrate the variations that can be introduced by simply remounting the aluminum plate on the holder in preparation for measuring the dynamic response. C-clamps are used for this process. Variations in the tightness or positions of the clamps apparently warp the plate enough to cause measurable changes in tile response. The third plot shows the response after stressing the tile/SIP system the first time. The fourth plot shows the response after remounting. The fifth plot shows the tile response after stressing the tile/SIP system the second time.

The dominant flexural mode shifts downward in frequency by 35 to 50 Hz each time the tile/SIP system is stressed. Although changes in rigid body modes are evident after the tile has been stressed, no clear characterization of the changes has yet been discovered.

Modeling

Modeling of the tile/SIP system is necessary to gain an understanding of the observed phenomena and to predict behavior under various inspection conditions. Without a model, there is less confidence in the bond condition inferred from empirical evidence because the evidence is not understood in the sense that the underlying physics is unknown. Interpreting unusual or unexpected behavior and predicting behavior under new circumstances are less accurate when the physics is unknown. An inspection system designed to operate only on empirical evidence would be more complex and more expensive than one based on knowledge of the physics of tile vibration.

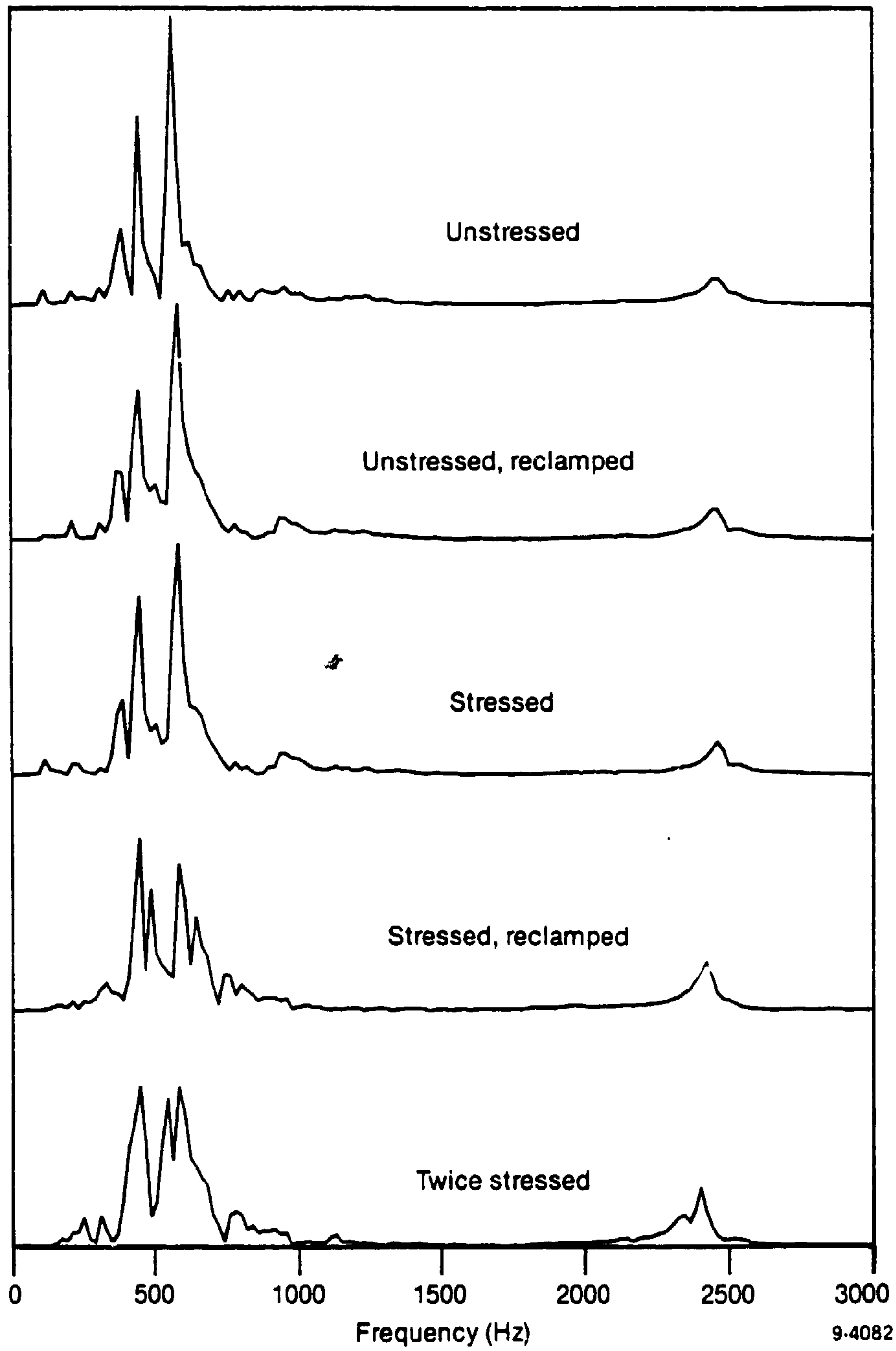

Figure 21. SIP aging.

Tile vibrational response data that have been collected display many characteristics that cannot be explained at this time. Explanations are usually sought in terms of resonance mode behavior. The following are a few unresolved issues regarding resonance mode behavior that a successful model could help solve:

- What modes are most affected by unbonds? Which are affected by changes not related to bond condition? How can we tell them apart?

- What complicating nonlinearities affect tile vibrational behavior?

- How can particular modes be excited or otherwise examined apart from all other modes?

- How many significant modes exist?

- How are different resonance modes coupled?

- What is the nature of the damping in the tile/SIP system? Is it linearly proportional to velocity, or more complicated in nature?

Answers to these and other questions about the physics of tile vibration would aid immensely the effort to interpret the physical data and determine bond condition. For example, a model might indicate that a particular mode is affected much more than others by unbonds. If a way could be found to examine that particular mode (the model might suggest a way) and determine its amplitude, frequency, and damping rate, it might then be possible to definitively identify unbonds.

The modeling effort has so far been limited to evaluation of two preliminary models. The first is based on simple assumptions about damping and the relationships between modes. This model predicts only the general form of modal behavior, as will be discussed below, rather than actual response to a given excitation. The physics of the tile/SIP system does not explicitly enter into this model. A second model was investigated that does consider the physics of the tile/SIP system. The details of this model are also discussed below.

The model of general modal behavior predicts that tile response can be represented as the sum of several damped harmonic oscillators, i.e.

$$v(t) = \Sigma A_n e^{-\alpha_n t} \cos(\omega_n t+\phi_n).$$

This prediction is based on the following assumptions about the physics of the tile/SIP system:

- The various resonance modes are uncoupled (there is no energy transfer between modes).

- Damping of each mode is linearly proportional to velocity.

The model was evaluated by comparing its predictions with experimental data. A sophisticated algorithm[2] was implemented for estimating the parameters (amplitude, damping rate, frequency, phase) of the resonance modes represented in the above equation. The results indicated that the model is too simple. A good fit could not be made to the data unless far more terms (50 or more) were included than seems reasonable. Also, small changes in the data resulted in large differences in the estimated resonance mode parameters.

Had this modeling attempt met with more success, a high resolution resonance mode identification technique would have resulted. The goal of being able to identify and track individual modes would have been realized. Although unsuccessful, the attempt has definitely resulted in a better understanding of tile vibrational response.

The second modeling study involves primarily the mathematical analysis of a very simplified physical representation of the tile/SIP system. The approach is to treat the tile/SIP as a system of coupled harmonic oscillators and use Lagrangian mechanics with generalized coordinates to set up the equations of motion. This reduces to determining expressions for the kinetic (T) and potential (U) energy of the coupled oscillators, calculating the Lagrangian (T-U), and then applying the Lagrangian equations of motion. The solutions to the coupled differential equations that result will define the eigen frequencies (i.e., resonances) of the system.

For illustration consider the simple case where a plate of mass M is supported at its corners by four identical springs. In this simple model the plate is constrained to piston like motions along the x3 axis and two rocking modes about two orthogonal axes, x1 and x2. For this system the generalized coordinates are x3, θ, and ϕ, where θ and ϕ are the angles of the rocking motions. If the plate has dimensions of 2A and 2B, the Lagrangian equations of motion are:

$$x_3'' + \frac{4k}{M} x_3 = 0$$

$$\frac{MB^2}{3} \theta'' + 4KB^2\theta = 0$$

$$\frac{MA^2}{3} \phi'' + 4KA^2\phi = 0$$

Assuming solutions of the form $x_i = A_i e^{-j(\omega_i t + \delta)}$, this system of coupled equations yields eigen frequencies of:

$$\omega_x = \sqrt{\frac{4K}{M}} \qquad \omega_\theta,\ \omega_\phi = \sqrt{\frac{12K}{M}} .$$

This analysis predicts that the two rocking modes are degenerate and higher in frequency than the fundamental piston mode by a factor of 1.73. Intuitively one can see where a change in the spring arrangement to simulate an unbond would break this degeneracy and create three distinct motions. It also predicts that the frequencies for a given mode should scale as

$$\frac{1}{\sqrt{M}} .$$

This seems to be born out in the analysis of data from tiles of differing mass. Table 1 shows how masses and frequencies compare for the mode of highest frequency on several different tiles. The mode of highest frequency is used as it is difficult to identify common modes between tiles. By using the highest frequency peak, some consistency is introduced. The first tile in the table (8122) is used as a baseline to calculate an artificial spring constant used in the calculations for the other three tiles. The observed discrepancy in tile 8387 is being investigated, but the agreement for tiles 9075 and 8491 is quite good.

The value of this method in modeling the tile vibration is yet to be proven, but it does provide a possible approach. Obviously this model does not incorporate the flexural modes. The complexities of the real situation will ultimately require a more realistic model. The SIP is known to be a nonlinear spring, for example. Nonetheless, useful information may still be obtained from this approach. The intent in this phase of the work is only to explore and identify possible model approaches, which can then be pursued, as appropriate, in subsequent phases.

TABLE 1. VARIATIONS IN RIGID BODY VIBRATION FREQUENCY WITH CHANGES IN MASS

		Highest Mode Frequency (Hz)	
Tile Number	Mass (g)	Estimated	Observed
8122	141	660	660
9075	183	581	577
8387	200	554	589
8491	275	472	470

FIELD TESTS

The field tests that were conducted in July of 1988 verified that tile resonances were detectable in the Orbiter Processing Facility (OPF) environment. However, the measurements, which were made on the Orbiter Columbia, also showed that the sensor response was complicated by ambient motion of the orbiter. While small (~10 μm at 20 Hz), these motions were also detected by the sensor and frequently masked the induced excitation. Because of this a fieldable system will require either modification of the sensor or modification of how the resonance information is extracted with the existing sensor. Details of these options are given below and an evaluation of these approaches is being conducted as part of ongoing work.

The field tests established that the vibration isolation of the sensor system, the long focal length optics, and the excitation methods could function in a field environment. There was no difficulty in obtaining an adequate reflection from the normal tile surfaces, and the pneumatic tires on the cart carrying the laser provided sufficient vibration isolation for the system.

There are at least two approaches to overcoming the difficulty caused by the ambient motion of the orbiter. The first would be to modify how the data are analyzed so that the sensor nonlinearities do not obscure the desired information. This would be possible because the large-amplitude ambient vibrations do not change the physics of how the bond affects the tile's dynamic response; a different measurement technique may be required, but the effect is still there. Some examples of such a modification would be to confine the analysis to the first 5 ms after excitation or to measure peak amplitudes of resonance vibrations induced by a CW tone. This latter technique was actually used during the field test at selected resonances. The second approach would be to continue sensor development to obtain a sensor that is linear over the required range of vibrations. The approach taken to date has been to use the existing sensor capability unless and until it is necessary to expend additional resources to build a heterodyne sensor. With this type of sensor the ambient vibration would just be filtered out. These and other possible approaches are being evaluated.

One of the most significant results of the field tests is that the response of the tiles on the Orbiter was similar to that observed in the laboratory. While it was not possible, nor was it the intent, to vary bond conditions on the tiles examined, it was possible to excite resonances and measure their existence with the acousto-optic sensor in a different fashion than the standard data collection method. Quantification of the ambient vibrations of the OPF environment was also significant as their impact can now be incorporated into any subsequent design of analysis techniques and/or sensors. In short, the field tests have provided definite evidence that will guide both the analysis and sensor design.

CONCLUSIONS FROM PHASE II WORK

Phase II of this project had two basic objectives. The first was to continue development of the sensing technology to the point where preliminary field measurements on the Orbiter could be made. This goal was achieved, thanks in large part to the development of the long focal length optics. Valuable information was obtained from the field experiments that clearly identifies areas where future efforts should be made.

The second goal was to advance the state of understanding of the physics of tile vibration and vibration measurement to the point where an informed decision could be made whether or not this approach is viable for field detection of real flaws on the Orbiter TPS. This goal was also achieved; concentrating on the pedigree tiles, a number of quantifiable unbond signatures were identified.

The following conclusions summarize the results of Phase II work on this project:

1. Vibration signatures associated with bond flaws are significant, repeatable, and consistent between similar tiles with similar bond flaws.

   A number of promising bond flaw signatures have been identified. These signatures are quantifiable and consistent among the pedigree tiles. Signatures include frequency and time domain features of the dynamic response as well as symmetry observations.

2. The measurement techniques developed for this project work in a field environment.

   An optical table is not required to make extremely sensitive displacement measurements; the sensor can operate in normal workplace "noise."

3. Modifications to the sensor or to analysis techniques are necessary to accommodate the large ambient motion present in some areas of the orbiter.

The field tests revealed that the ambient vibration of the orbiter is too large for the current sensing method and/or analysis techniques. The current sensor is very good at sensing vibrations with peak-to-peak amplitudes less than 0.5 μm. Motions greater than 13 μ were measured in some areas of the orbiter during the field tests.

RECOMMENDATIONS FOR PHASE III WORK

Knowledge gained during Phase II clearly indicates the course of work necessary to convert this technology into an inspection tool for regular use in an operational environment. Modifications to the current sensor are needed to provide the capability to obtain measurements from all areas of the Orbiter. Laboratory work with a broader variety of tiles is required to extend the current understanding of unbond effects on tile response. A serious modeling effort is needed, in conjunction with the laboratory work, to understand the physics of tile vibration phenomena. And, finally, hardware and software that are compact and easy to operate must be designed and developed.

The following is a description of proposed Phase III work broken down into tasks:

1. Requirements Definition - Present a universe of possibilities of how a system might function to be added to, subtracted from, or otherwise enhanced by NASA and their designated contractors. The output will be a specification for a prototype system and a concept for how it will be used in the OPF.

2. Model Phenomena - Construct, buy, or otherwise obtain useful models for both the rigid body and flexural modes. Use these to study representative tiles and bond situations. Verify models with experimental measurements. Minimum utility is defined by the models' ability to predict spectral changes due to bond condition. It would also be desirable (but not necessary) for them to predict sensitivities, coupling effects, and effects of tile-to-tile variations.

3. Design and Fabrication of Signal Analysis Hardware - Convert the DEC system to a compact field version that includes all data acquisition and analysis capabilities. Make provisions for tie in to Kennedy Space Center's (KSC) tracking systems. Determine all other hardware aspects necessary to meet design requirements.

4. Optics Design and Fabrication - Evaluate and select final laser technique. Resolve issues such as how to autofocus, vibration isolation, and physical layout. Ensure compatibility with other subtasks and all safety regulations at KSC.

5. Prototype Trials - Conduct tests at KSC and INEL to shakedown the system. Use at KSC will include the development of a database on as-bonded tiles and replacements. In conjunction with KSC, write and implement preliminary operating procedures and evaluate how the measurement process integrates into the workflow.

6. Final Revisions and Report - Based on the prototype trials, rework any weak areas in the design, document the design for subsequent models, and present final report.

REFERENCES

1 P. O. Cooper and J. W. Sawer, "Life Considerations of the Shuttle Orbiter Densified-Tile Thermal Protection System," (reprint supplied by NASA).

2. R. Kumaresan and D. W. Tufts, "Estimating the Parameters of Exponentially Damped Sinusoids and Pole-Zero Modeling in Noise," IEEE Transactions on Acoustics, Speech, and Signal Processing, Vol. ASSP-30, No. 6, December 1982.